Chem Soc Rev

Thermodynamic and Kinetic Hydricities of Metal-Free Hydrides

Thermodynamic and Kinetic Hydricities of Metal-Free Hydrides

Stefan Ilic[‡], Abdulaziz Alherz[♭], Charles B. Musgrave[♭ §#], Ksenija D. Glusac[‡*]

[‡]Department of Chemistry, University of Illinois at Chicago, Chicago, IL 60607, United States

[‡]Chemical Sciences and Engineering Division, Argonne National Laboratory, Lemont, IL 60439, United States

[♭] Department of Chemical and Biological Engineering and [§]Department of Chemistry and Biochemistry, University of Colorado, Boulder, CO 80309, United States

[#]Materials and Chemical Science and Technology Center, National Renewable Energy Laboratory, Golden, CO 80401, United States

Abstract

Metal-free hydrides are of increasing research interest due to their roles in recent scientific advances in catalysis, such as hydrogen activation with frustrated Lewis pairs and electrocatalytic CO_2 reduction with pyridinium and other aromatic cations. The structural design of hydrides for specific applications necessitates the correct description of their thermodynamic and kinetic prowess using reliable parameters – thermodynamic hydricity (ΔG_{H^-}) and nucleophilicity (N). This review summarizes reported experimental and calculated hydricity values for more than 200 metal-free hydride donors, including carbon-, boron-, nitrogen- and silicon-based hydrides. We describe different experimental and computational methods used to obtain these thermodynamic and kinetic parameters. Furthermore, tabulated data on metal-free hydrides are discussed in terms of structure-property relationships, relevance to catalysis and contemporary limitations for replacing transition-metal hydride catalysts. Finally, several selected applications of metal-free hydrides in catalysis are described, including photosynthetic CO_2 reduction and hydrogen activation with frustrated Lewis pairs.

I. Introduction

Hydride donors are powerful reducing reagents. By transferring a hydride ion to the appropriate substrate, hydride donors achieve a two-electron, proton-coupled reduction in a concerted fashion, without the formation of high energy, often unstable, intermediates. Transition metal hydrides, particularly those made of the noble metals Rh, Pd and Pt, are generally excellent hydride donors and can often be used in catalytic amounts through either electrochemical or chemical regeneration of the hydride donor from its conjugate hydride acceptor.[1-3] However, due to the low abundance and high toxicity of transition metal-based hydrides,[4] recent scientific efforts have investigated metal-free hydride donors and their utilization in catalytic reduction processes.

Initial interest in metal-free hydride donors (Scheme 1a) was motivated by their close resemblance to enzymatic cofactors, nicotinamide adenine dinucleotide phosphate (NADPH) and flavin adenine dinucleotide (FADH$_2$). Natural systems often utilize these organic hydride donors to drive a myriad of reduction reactions. For example, the critical step in CO_2 reduction in photosynthetic systems is a hydride transfer from reduced NADP (NADPH),[5] a carbon-based hydride donor with moderate hydride donating ability. Inspired by natural cofactors, several synthetic analogs were investigated, such as Hantzsch esters, and applied as mild hydride sources in various asymmetric transformations, often activated by the presence of a metal ion in a similar fashion as in natural enzymatic systems.[6] Furthermore, stronger hydride donors (e.g. Super hydride[TM], lithium triethylborohydride, Scheme 1a) are often used as stoichiometric reagents for reductions of numerous functional groups, such as C=O, C=N and C=C bonds in organic synthesis.[7, 8] More recently, significant progress has been made towards the catalytic use of metal-free hydride donors. Specifically, frustrated Lewis pairs, made of sterically-hindered hydride and proton acceptors, have emerged as a promising class of metal-free catalysts for hydrogen activation.[9, 10]
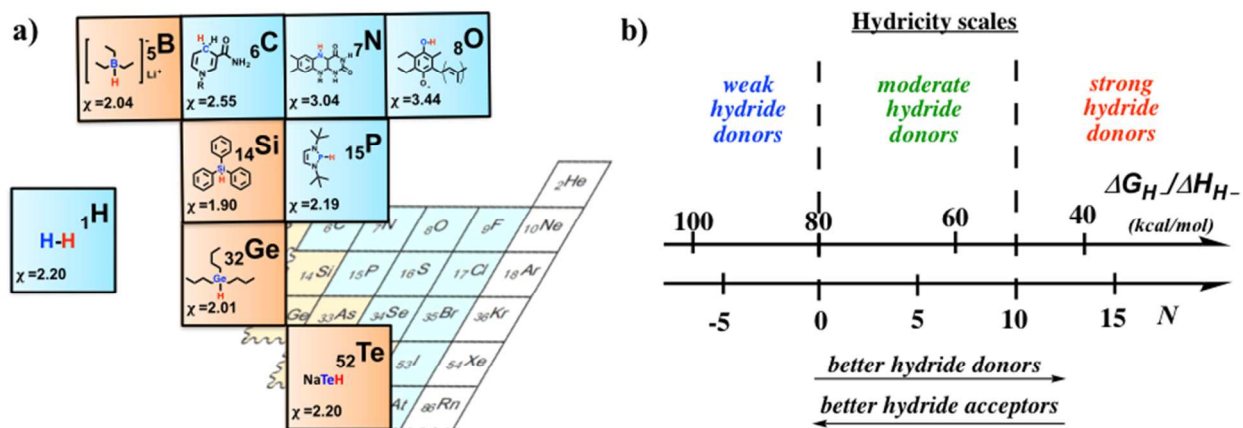
Scheme 1. a) Some examples of metal-free hydride donors. Metalloids are shown in orange, while nonmetals are shown in blue. Hydridic hydrogens are shown in red and electronegativity values are represented by "χ". The selected examples of each group are presented as follows, from top left: boron (lithium triethylborohydride, Super hydride^{TM8}), carbon (NADPH,[11] R = adenine dinucleotide phosphate), nitrogen (FADH$_2$,[12] R = adenine dinucleotide), oxygen (coenzyme Q$_{10}$[13]), silicon (triphenylsilane[14]), phosphorus (2-H-diazaphospholene[15]), germanium (tributylgermane[16]) and tellurium (sodium hydrogen telluride[17]). b) Thermodynamic and kinetic hydricity scales used to evaluate hydride donor ability and reactivity of metal-free hydride donors.

The hydridic H-atom in metal-free hydrides is bound either to a nonmetal - carbon, nitrogen, oxygen or phosphorus - or a metalloid - boron, silicon, germanium or tellurium (Scheme 1). In general, the hydride donating ability of metal-free hydrides can be tuned over a wide range by varying the donor's electronic and/or structural parameters, such as the polarization of the hydridic bond of the hydride donor or the extent of positive charge delocalization in the conjugate hydride acceptor. The selection of appropriate hydride donors for various desired applications is usually made by considering thermodynamic and kinetic hydricity parameters. The thermodynamic hydricity (ΔG_{H-}) is defined as the standard Gibbs free energy change for the dissociation of a hydride donor R-H into a conjugate hydride acceptor R$^+$ and a hydride anion H$^-$:

$$R - H \ \rightarrow \ R^+ \ + \ H^- \qquad\qquad \Delta G_{H-} \qquad\qquad\qquad (1)$$

ΔG_{H-} values are always positive because spontaneous heterolytic dissociation of the hydride does not occur and lower values for ΔG_{H-} indicate a better hydride donor (Scheme 1b). Based on their ΔG_{H-} values in acetonitrile (MeCN) and dimethyl sulfoxide (DMSO), hydrides can be divided into weak (ΔG_{H-} > 80 kcal/mol), moderate (50-80 kcal/mol) and strong (< 50 kcal/mol) donors. The Gibbs free energy associated with the reverse of process (1) is defined as the hydride affinity of R^+, where this parameter is relevant for oxidation reactions involving abstraction of hydride ions from relevant substrates. Naturally, the ΔG_{H-} of the hydride donor and the hydride affinity of the conjugate hydride acceptor have the same value, but with opposite signs.
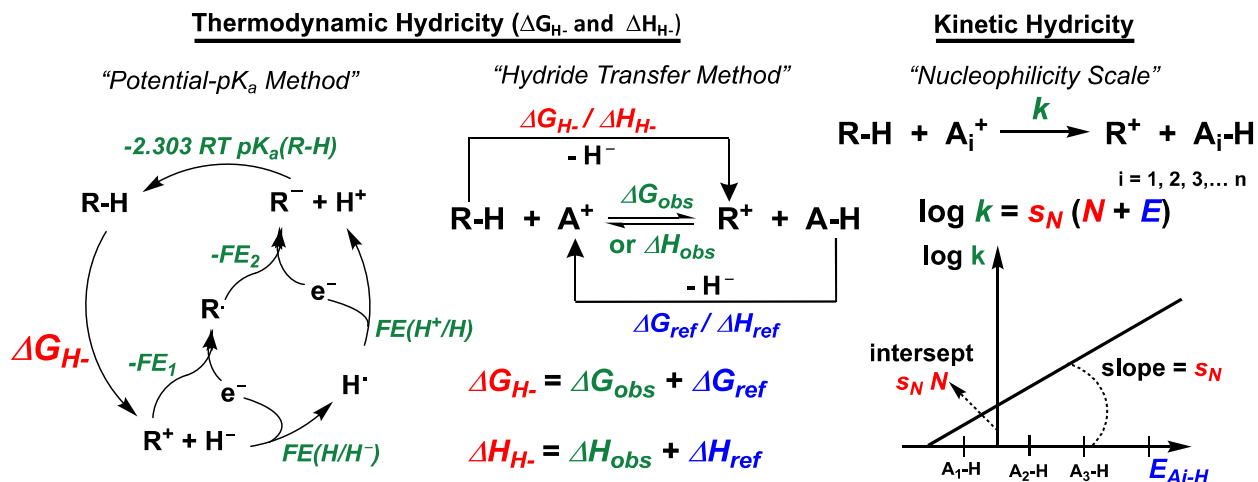
Kinetic hydricity of metal-free hydride donors is often defined in terms of a nucleophilicity factor N, which is a purely empirical parameter obtained from experimental rates for hydride transfer reactions with reference acceptors. The N value of the hydride donor can be correlated directly with the activation free energy for the hydride transfer reaction with an acceptor.[18, 19] Therefore, N can be used to quantify the kinetic strength of a hydride donor, where stronger hydride donors are defined to possess larger N values (Scheme 1b). Hydride donors can be divided into slow reacting (N < 0), moderately reactive (0 – 10) and highly reactive (> 10).

A number of exhaustive reviews have covered metal-free hydride motifs and their application in organic synthesis and photoelectrocatalysis.[6, 10, 20, 21] Here, we approach metal-free hydrides from the mechanistic perspective; to explain the driving forces and kinetics of hydride transfer in natural and artificial reduction processes, we review the literature reports of thermodynamic and kinetic hydricities of metal-free hydride donors. The first two sections summarize different experimental and computational methods for their determination, as well as a description of the advantages and disadvantages of each approach. The reported hydricity parameters are then tabulated, and the data used to derive structure-property relationships of the hydrides, with a focus on trends that govern the thermodynamic and kinetic properties for different classes of metal-free hydride donors. Next, we analyze the tabulated hydricities and other electrochemical properties to evaluate the applicability of metal-free hydrides to catalytic processes, such as hydrogen activation and solar fuels generation. In the last section, several selected examples of hydride transfer processes are described to illustrate the application of the hydricity concept to natural and artificial reduction reactions.

II. Experimental Methods

Several different experimental approaches are utilized to evaluate hydride donating abilities of metal-free hydrides. The Gibbs free energy ΔG_{H^-} is the most accurate parameter to evaluate the thermodynamic driving forces for hydride transfer reactions. Two main experimental approaches are used to obtain ΔG_{H^-} for metal-free hydride donors: the "potential-pK_a" and "hydride transfer" methods (Scheme 2). However, both methods are often experimentally challenging. To avoid these challenges, one can resort to obtaining the experimental enthalpy change (ΔH_{H^-}) and assume that the entropic contributions to the hydride transfer processes are insignificant. Although this assumption is not always valid, the determination of ΔH_{H^-} is experimentally simple, which enables one to screen a large number of model compounds. In addition to these thermodynamic parameters, a kinetic nucleophilicity scale was developed by Mayr,[18, 19] in which the nucleophilicity N of metal-free hydrides is derived from experimental rates for the relevant hydride transfer reactions. Although the nucleophilicity scale does not provide absolute activation barriers (because it is expressed relative to the electrophilicities of reference hydride acceptors), it provides valuable information regarding the relative reactivity of various hydrides. The governing principles, as well as the advantages and disadvantages of each method are discussed below. Additionally, this section provides an exhaustive tabulation of the previously reported experimental hydricity parameters for metal-free donors.

Scheme 2. Illustrative description of the methods used to obtain thermodynamic and kinetic hydricities. The desired values obtained as outcomes from these methods are represented in red; measured parameters are represented in green and reference values are represented in blue.

Thermodynamic Hydricity (ΔG_{H-} and ΔH_{H-}) **Kinetic Hydricity**

"Potential-pK$_a$ Method" *"Hydride Transfer Method"* *"Nucleophilicity Scale"*

$$\Delta G_{H-} / \Delta H_{H-}$$

$$-2.303\ RT\ pK_a(R\text{-}H)$$

$$R\text{-}H \quad\quad R^- + H^+$$

$$-H^-$$

$$R\text{-}H + A^+ \underset{\text{or } \Delta H_{obs}}{\overset{\Delta G_{obs}}{\rightleftharpoons}} R^+ + A\text{-}H$$

$$R\text{-}H + A_i^+ \xrightarrow{\ k\ } R^+ + A_i\text{-}H$$

$$i = 1, 2, 3,... n$$

$$\log k = s_N (N + E)$$

$$-FE_2$$

$$R^\cdot$$

$$e^-$$

$$FE(H^+/H)$$

$$-H^-$$

$$\Delta G_{ref} / \Delta H_{ref}$$

$$\Delta G_{H-} \quad -FE_1$$

$$e^-$$

$$H^\cdot$$

$$R^+ + H^- \quad FE(H/H^-)$$

$$\Delta G_{H-} = \Delta G_{obs} + \Delta G_{ref}$$

$$\Delta H_{H-} = \Delta H_{obs} + \Delta H_{ref}$$

log k

intersept $s_N N$ slope = s_N

A_1-H A_2-H A_3-H $E_{Ai\text{-}H}$

The Potential-pK$_a$ Method. The "potential-pK$_a$" method is based on a thermochemical cycle that treats the free energy of hydride transfer as the net free energy of two electron transfers and a proton transfer, where the ΔG_{H^-} values are obtained from the relevant one-electron reduction potentials E_1 (for $R^+/R^\cdot$) and E_2 (for $R^\cdot/R^-$), and pK_a value of R-H (Scheme 2). To close the thermochemical cycle, the standard two-electron reduction potential of a proton ($\Delta G_{H+/H-}$) needs to be evaluated using the reduction potentials $E(H^+/H)$ and $E(H/H^-)$ (Scheme 2). The proton reduction potential $\Delta G_{H+/H-}$ in MeCN and DMSO have been evaluated previously by Parker ($\Delta G_{H+/H-}(MeCN)$ = 54.7 kcal/mol, $\Delta G_{H+/H-}$ (DMSO) = 69.9 kcal/mol),[22] and these values were used to derive experimental thermodynamic hydricities of both metal-based[23-35] and metal-free[22, 36-40] hydride donors. However, it is important to emphasize that the evaluation of $\Delta G_{H+/H-}$ requires a number of assumptions associated with the solvation of a proton, hydrogen atom and hydride ion. For example, the solvation free energy of a proton is derived from its aqueous value and the free energy to transfer the proton from water to the solvent of interest, while the solvation of a hydrogen atom is approximated as the solvation free energy of helium.[41] Furthermore, $E(H/H^-)$ is estimated using its aqueous value and the free energy to transfer a hydride from water to an organic solvent, which is obtained from linear correlations of halide ions.[37]

The potential-pK$_a$ approach has been applied by us[40] and others[22, 36-39] to obtain the thermodynamic hydricities of relatively weak organic hydride donors, such as arylmethanes, anthracene, fluorenes, quinones and acridines (Table 2). However, a number of experimental challenges have limited the broader use of the "potential-pK$_a$" method. For instance, the standard

reduction potentials E_1 and E_2 cannot always be practically obtained experimentally, either because the reduction peaks are chemically irreversible on cyclic voltammetry timescales or because the reduction processes occur outside the solvent electrochemical stability window. The latter issue is particularly important for species associated with strong hydride donors, because there is a linear correlation between the first reduction potential and thermodynamic hydricity (as discussed in Relevance to Catalysis section). For cases where chemical irreversibility is an issue, some researchers approximate the standard reduction potentials using the cathodic peak potentials, which introduces an ~0.3 V error in the estimated reduction potentials (assuming that the irreversibility occurs at the 100 mV/s sweep rate due to a subsequent chemical reaction with a rate constant of 10^{10} s^{-1}).[42-44] In some cases, square-wave voltammetry is used to obtain a more accurate approximation of the standard reduction potentials.[45-48] In cases where the first reduction is chemically irreversible, the second reduction process does not occur and will not be observed in the cyclic voltammograms. In such cases, the second reduction potential can be obtained by performing the one-electron oxidation of the deprotonated hydride, R$^-$.[49] Alternatively, hydride donor ability of metal-free hydrides can be experimentally evaluated using the standard reduction potential for proton-coupled conversion of R to RH$_2$.[50-52]

Another challenge associated with the potential-pK$_a$ method is that metal-free hydrides tend be very weak acids, and the determination of their pK_a values is often hindered by the pK_a of solvent (pK_a(DMSO) = 35,[53] pK_a(ACN) = 33[54]). On average, metal-free hydride donors are weaker acids than metal-based hydrides. For example, the pKa values of [Ni^{II}-H]$^+$ hydride donors in acetonitrile are in the 13-24 range,[55] while the pKa values of acridine-based hydrides are in the 27-50 range.[40] For hydrides that are more basic than the solvent, the relevant pK_a values can be obtained using extrapolation techniques.[53]

The Hydride Transfer Method. In cases where the potential-pK$_a$ method cannot be applied, the "hydride transfer" method provides an excellent alternative approach. This method involves the determination of the equilibrium constant for the hydride transfer (HT) reaction between a donor of interest (R-H) and a reference acceptor with known hydride affinity (A$^+$, Scheme 2). The equilibrium concentrations are readily obtained using NMR or UV/Vis absorption spectroscopy, and the "hydride transfer" method has been successfully applied to a series of metal-free hydride

donors: NADH analogs,[40, 56] imidazole analogs,[40] acridine analogs[40, 56] and triethylborohydride.[57] It is important to mention that the accuracy of this method requires that the equilibrium of the hydride transfer reaction is reached before the concentrations are measured. This condition implies that the ΔG_{H-} of A-H needs to be within 2-3 kcal/mol of the thermodynamic hydricity of R-H, indicating that usually several hydride acceptors A^+ need to be tested before the appropriate reagent is identified. To ensure that equilibrium has been obtained, a second equilibrium of the reaction mixture should be obtained by adding products to the equilibrated system and the equilibrium constant re-measured.[1] In some cases, equilibrium is reached only after several weeks, increasing the probability that an undesired side reaction will occur. Alternatively, the equilibrium constant for the hydride transfer reaction can be obtained by measuring the rate constants for the forward and reverse reactions between a hydride of interest and a reference hydride. This approach has been particularly utilized in early studies on hydride transfer between NADH analogs.[51, 58-60]

Other Methods. The thermodynamic hydricity of transition metal hydrides is often determined using the "H_2 heterolysis" method, where the equilibrium constant for the heterolysis of H_2 is measured in the presence of a hydride acceptor (R^+) and the appropriate base (B) to make the hydride R-H and protonated base B-H$^+$.[28, 29, 61-66] However, the H_2 heterolysis method has not been utilized to derive ΔG_{H-} values of metal-free hydrides, even though reversible H_2 splitting has been observed for a number of frustrated Lewis pairs.[9, 67-71]

Given the numerous technical difficulties associated with the determination of ΔG_{H-}, it is often more convenient to instead determine the enthalpic hydricity (ΔH_{H-}). In this method, the heat released during a hydride transfer reaction between a hydride donor of interest (R-H) and the hydride acceptor A^+ with known hydride affinity is measured using calorimetry (Scheme 2). Using this approach, Cheng and coworkers determined ΔH_{H-} values for a large number of organic hydride donors, which enabled the derivation of structure-property relationships for these model compounds.[45-48, 72-76] Furthermore, ΔH_{H-} can be obtained using the H_2 heterolysis method, as was demonstrated for B(C$_6$F$_5$)$_3$ by measuring the heat released during H_2 cleavage in the presence tri-tert-butylphosphine base.[77] The main assumption that accompanies the use of ΔH_{H-} values is that the entropic contribution to ΔG_{H-} is either negligible or constant across different hydride donors. While this assumption is justifiable for some series of structurally similar

hydrides, the difference between the enthalpy change and the room temperature Gibbs free energy change varies within the 4 - 12 kcal/mol range (see Structure-Property Relationship section).

Nucleophilicity. In addition to the thermodynamic parameters discussed above, Mayr developed a nucleophilicity scale, which evaluates the relative kinetic reactivity of hydride donors.[19, 78-82] This method involves the experimental determination of rate constants (k) for a reaction between a hydride donor of interest and a series of hydride acceptors with known electrophilicities (E). The results are fit to the following expression:

$$\log k = s_N (N + E) \qquad (2)$$

which enables the determination of the parameters N and s_N. The nucleophilicity parameter (N) describes the rate of hydride transfer by a hydride donor. The experimentally obtained N values for metal-free hydrides range between -5 and 15, where the larger values indicate a more kinetically active hydride donor. The parameter s_N is the sensitivity parameter of a donor whose values range between 0.5 and 1.2. The sensitivity parameter depends on the structural characteristics of hydride donors and is expected to be similar over the same class of compounds.

The nucleophilicity parameter is set to a relative scale where the values are defined using bis(p-methoxyphenyl)methyl cation as a reference electrophile, whose E parameter is set to 0, and a reference nucleophile (2-methyl-1-pentene), whose s_N parameter is set to 1.[18, 83] Furthermore, the nucleophilicity scale is highly empirical and does not provide direct information about the thermodynamic and kinetic parameters related to the hydride transfer process. Despite these drawbacks, the nucleophilicity scale provides valuable information about the relative nucleophilicities of hydride donors that can guide the selection of a metal-free hydride that will be most suitable for a reaction of interest.

III. Computational Methods

Computational quantum chemical methods are a fast and inexpensive alternative to experimental approaches for determining hydricity that also provide a fundamental and detailed description of the phenomena involved in the hydride transfer process. The calculated hydricity parameters often accurately correlate with the experimental results, thus enabling their quantum chemical prediction for species whose empirical values are not known. This is especially useful when the hydrides of interest include species that are difficult to synthesize, expensive or in cases where the hydricity of a species has been measured in one solvent, but has not yet been measured in the solvent of interest. The thermodynamic hydricities of a wide variety of metal-free hydrides have been calculated in MeCN and DMSO, and representative values are listed in Table 2. The ΔG_{H-} values are calculated using one of two approaches: (i) the direct approach, where thermodynamic hydricity is calculated from absolute Gibbs free energies of individual species (G_{R-H}, G_{R+} and G_{H-});[84-86] and (ii) indirect approaches, which are analogous to the experimental "hydride transfer" and "potential-pK$_a$" methods,[87-92] described in the Experimental methods section above. In addition to the thermodynamic hydricities, the kinetic nucleophilicity parameter N can also be derived computationally from transition state energies for hydride transfer reactions.[93] This section describes each computational method in detail, including a discussion of the advantages and challenges associated with each approach.

The Direct Approach. In the direct approach, ΔG_{H-} values of hydrides (R-H) are determined from absolute Gibbs free energies using the following equation:

$$\Delta G_{H^-} = G(R^+) + G(H^-) - G(RH) \qquad\qquad (3)$$

Gibbs free energies of the solvated hydride donor, *G(RH)*, and the corresponding cation, *G(R$^+$)*, can be calculated with exquisite accuracy using quantum chemical methods.[94-96] However, the Gibbs energy associated with the solvated hydride ion, *G(H$^-$)*, represents a computational challenge. Most commonly employed implicit solvation models, which describe the solvent as a continuous polarizable medium, only account for electrostatic interactions and neglect dispersion and repulsion, as well as hydrogen-bonding between the solute and solvent molecules,[97-101] thus

yielding inaccurate solvated hydride ion energies. These inaccuracies are especially significant for the solvated hydride ion modeled by some polarizable continuum models (PCM) based on united-atom force field methods as they do not assign cavities for hydrogen atoms.[97] For example, Papai and coworkers reported obtaining a free energy of −387.8 kcal/mol for the solvated hydride in an implicit MeCN solvent model, which they determined was inaccurate compared to their empirically derived value of −404.7 kcal/mol.[102] The solution to this problem is to treat solvents explicitly by directly including solvent molecules in the model. This still requires an approximation for the solvent environment as only a relatively small number of solvent molecules can be explicitly included in the quantum mechanical model. A further improvement on the model involves using a hybrid implicit/explicit approach, where the solute is solvated by a shell of quantum-mechanically treated solvent molecules embedded in implicit solvent.[97, 103-105] Both of these approaches reduce the errors that arise from solvation by more correctly describing the solute-solvent interactions, but require considerably more computationally expensive calculations as the number of electrons increases with additional quantum-mechanically described solvent molecules in the model.[106] To the best of our knowledge, explicit solvent models have not yet been used to predict ΔG_{H^-} or hydride ion solvation energies. As we discuss below, other approaches are more efficient in predicting thermodynamic hydricities.

The challenge associated with calculating the solvation energy of the hydride ion can be circumvented by providing a semi-empirical value for $G(H^-)$ in the solvent of interest. The hydride ion has not yet been observed in common solvents such as water, MeCN, or DMSO, because of its tendency to react with protons to evolve molecular hydrogen. Consequently, the experimental value for $G(H^-)$ must be obtained using indirect methods. One such method is the scaling approach, in which $G(H^-)$ is obtained from equation (1), using experimental ΔG_{H^-} and the calculated absolute Gibbs free energies for R^+ and R-H.[86, 102, 107, 108] The $G(H^-)$ value is obtained as an intercept of the linear fit of experimental hydricities ΔG_{H^-} with respect to the sum defined as $\Delta G_{HHR} = G(R^+) - G(R\text{-}H)$, as shown in Figure 1. According to the equation $\Delta G_{H^-} = \Delta G_{HHR} + G(H^-)$, the slope of the line is expected to be unity. With a slope of unity, Papai and Nimlos were able to obtain values of $G(H^-)$ that minimize the errors in the predicted thermodynamic hydricities.[102, 109] However, the results of Muckerman et al. show that the best linear fit provides

a slope that deviates slightly from 1, and they associate this deviation to deficiencies in the implicit solvation model.[86] Nevertheless, the non-unity slope reproduced experimentally determined ΔG_{H^-} more accurately compared to the linear fit constrained to have unity slope. The scaling approach has been successfully utilized for calculations of several transition metal hydrides[107, 108, 110] and a metal-free dihydropyridine.[111] The advantage of the scaling approach is that it reduces systematic error because the fit is generated using multiple data points. A drawback of this approach is that the quality of the linear fit depends on it spanning a wide range of ΔG_{H^-} hydricities.
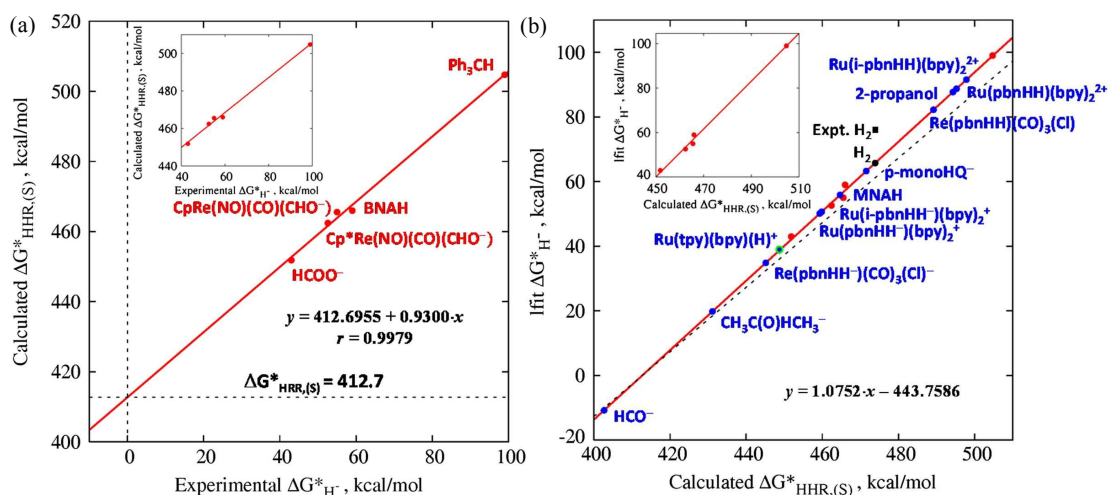

Figure 1. (a) Linear fit of the computed quantity ΔG_{HHR} (kcal/mol) versus the experimentally determined thermodynamic hydricity ΔG_{H^-} (kcal/mol) for the hydride species: HCOO⁻, BNAH, Ph₃CH, CpRe(NO)(CO)(CHO⁻), and Cp*Re(NO)(CO)(CHO⁻) in MeCN. A good correlation is obtained (r = 0.9979), with a slope (0.93) that deviates slightly from unity and an intercept − $G(H^-)$ = 412.7 kcal/mol. (b) The linear fit obtained in (a) is used to predict the hydricities ΔG_{H^-} of the species labelled in blue. Assuming a slope of unity clearly represents a poorer fit as indicated by the dashed black line. This method fails to predict the thermodynamic hydricity of H₂ due to difficulties in calculating the free energy of the proton. Reproduced from Ref. [86] with permission from the Royal Society of Chemistry.

$G(H^-)$ can also be obtained by computing the hydride ion gas-phase free energy $G(H^-)_{gas}$ and then accounting for solvation effects using derived solvation energies for the hydride ion (ΔG_{sol}):[40, 85]
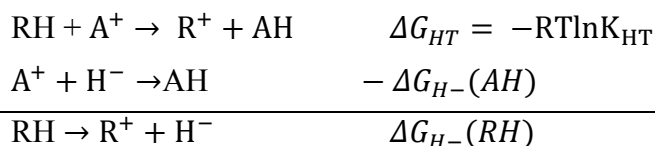
$$G(H^-) = G(H^-)_{gas} + \Delta G_{sol} \qquad (4)$$

The solvation energy ΔG_{sol} can be extracted from the experimental standard reduction potential for the hydride ion described in the Experimental methods section. The experimental reduction potentials (E_{H/H^-}) are available for a range of solvents,[22] enabling the evaluation of hydride solvation energies in MeCN, DMSO and water. This approach was shown to reproduce the experimental thermodynamic hydricities of several dihydroacridines.[40, 85] Table 1 lists absolute Gibbs free energies for the hydride ion $G(H^-)$ in MeCN obtained using the semi-empirical methods described above. While Table 1 lists a large spread of values ranging from –400.7 to –412.7 kcal/mol in MeCN, the calculated hydricities ΔG_{H^-} for model hydrides were all within 3 kcal/mol of the experimental values.[40, 85, 86, 102, 109] Creutz et al. estimated that $G(H^-)$ is expected to be 16 – 22 kcal/mol lower in water than in MeCN.[24]

Table 1. Summary of different $G(H^-)$ values obtained computationally via various approaches and levels of theory in MeCN.

LEVEL OF THEORY	APPROACH	GH- (kcal/mol)	REF
B3LYP/6-31+G(d,p)*/PCM	Scaling with non-unity slope	**−412.7**	86
B3LYP/6-31+G(d,p)*/PCM	Scaling with unity slope	**−406.6**	86
B3LYP/SDDP/PCM-UA0	Scaling	**−404.7**	102
wB97X-D/6-311+G(2df,p)/CPCM	Experimental Solvation Correction	**−402.9**	40, 85
B3LYP/SDD+631G(d)**// BLYP/SDD+6-31G(d) [PCM-UA0]	Scaling	**−400.7**	109

Indirect Approaches. Indirect methods do not require knowledge of the absolute Gibbs energy of the hydride ion. For example, the isodesmic approach is similar to the experimental "hydride transfer" method and involves the calculation of ΔG_{HT} for a hydride transfer reaction between the donor of interest and a reference acceptor, with known affinity.[87, 88]

$$
\begin{array}{ll}
RH + A^+ \rightarrow R^+ + AH & \Delta G_{HT} = -RT\ln K_{HT} \\
A^+ + H^- \rightarrow AH & -\Delta G_{H-}(AH) \\
\hline
RH \rightarrow R^+ + H^- & \Delta G_{H-}(RH)
\end{array}
$$

The isodesmic approach has been used extensively to determine the thermodynamic hydricities and affinities of metal-free hydride donors, such as arylcarbeniums, quinones, boranes and other main group hydrides.[88-92, 112] This indirect method is relatively simple because energies of the solvated hydride donors (R-H and A-H) and corresponding hydride acceptors (R^+ and A^+) can be readily obtained using quantum chemical calculations. However, because the isodesmic approach depends on the thermodynamic hydricity of the single reference hydride, any error in the ΔG_{H-} of the reference is systematically propagated to the ΔG_{H-} calculated via this approach. Another drawback of this method is that ΔG_{H-} can only be calculated for solvents which have a reliable reference molecule for which the hydricity has been determined. For instance, this approach is currently limited to only MeCN and DMSO solvents.

Another indirect method for calculating thermodynamic hydricities is analogous to the experimental "potential-pK_a" method described in the Experimental methods section. This computational method is semi-empirical, and involves quantum-chemical calculations of the standard reduction potentials E_1 and E_2 and acidity values (pK_a) of relevant species in the solvent of interest (see Scheme 2 for definition of E_1, E_2 and pK_a).[113] These calculated values are combined with the experimental standard reduction potentials for the hydride ion ($E_{H+/H-} = E_{H+/H} + E_{H/H-}$) in the solvent of interest using the equation shown in Scheme 2. Recently, these methods have been employed to predict the ΔG_{H-} of various transition metal hydrides in water.[113] The authors argue that the experimental determination of some aqueous ΔG_{H-} values can be hindered by inhibition of electrochemical and acidity measurements arising from solubility issues, and that computational methods can overcome these challenges.[114] However, the computational determination of aqueous ΔG_{H-} hydricities is challenging because experimental data for the comparison are not sufficiently available.

Calculated Nucleophilicity. Computational methods are also utilized to calculate the kinetic parameters, such as the nucleophilicity N discussed in the Experimental Methods section. Specifically, Alherz et al. showed that the kinetic nucleophilicity parameter of hydrides can be determined computationally via a linear fit between the activation free energy of a hydride transfer from a hydride donor to a hydride acceptor and the experimental nucleophilicity, as indicated by equations (5-6).[93]

$$k = \frac{k_{\mathrm{B}}T}{h} exp(-\Delta G^{\ddagger}/RT) \qquad (5)$$

$$N = -\frac{1}{2.3RTs_N}\Delta G^{\ddagger} + N_0 \qquad (6)$$

The transition state theory-based equation (5) is combined with Mayr's equation (2) to obtain equation (6).[18, 19] The linear relation between N and the activation free energy $\Delta G^{\ddagger}$ only holds if, 1) the hydride acceptor or 'electrophile' is constant for the hydrides considered and 2) the sensitivity parameter s_N is constant, which is a valid assumption within a class of hydrides.[19] The constancy of the electrophile can be ensured by examining the same hydride acceptor species for all HT reactions considered.[93] The limitations of the Mayr equation are described in more detail by Bentley.[115, 116] In accordance with the Bell-Evans-Polanyi principle, the free energies and enthalpies of reaction for HTs have also been shown by Alherz et al. to exhibit a linear correlation with the nucleophilicity within a class of hydride donors.[93, 117, 118] Others, such as Pratihar and Kiyooka,[119, 120] have developed empirical relationships that utilize thermodynamic properties, such as the chemical hardness and electron affinity, to predict the nucleophilicities and electrophilicities of various nucleophiles and electrophiles. These values can be used to predict the kinetic properties of hydride donors and hydride acceptors.

Table 2 summarizes calculated thermodynamic hydricities for a range of metal-free donors, including carbon-, boron-, nitrogen- and silicon-based hydrides. In general, very good agreement is observed between the reported experimental and calculated values obtained from various methods, as shown in Figure 2. The mean absolute deviation (MAD) between experimental and calculated ΔG_{H^-} was found to be 3.4 kcal/mol, and the root-mean-square error (RMSE) is 5 kcal/mol (MAD = 3.0, RMSE = 3.7, ignoring the two outliers). The MAD and RMSE for enthalpic hydricities were determined to be 1.4 and 1.8 kcal/mol, respectively.
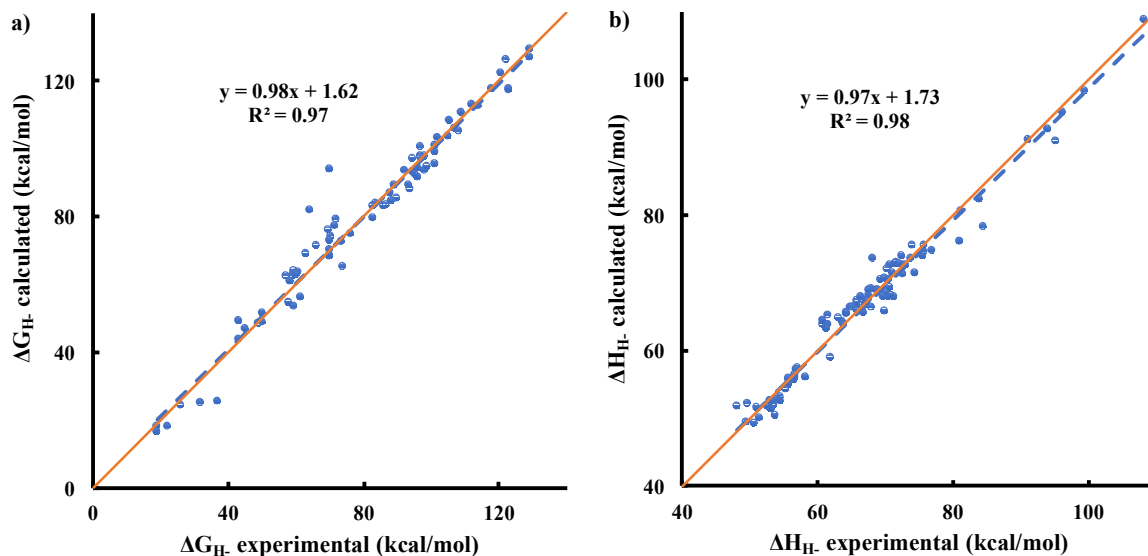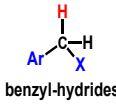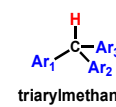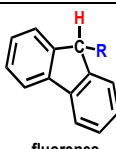
a)

ΔG_{H^-} calculated (kcal/mol)

y = 0.98x + 1.62
R² = 0.97

ΔG_{H^-} experimental (kcal/mol)

b)

ΔH_{H^-} calculated (kcal/mol)

y = 0.97x + 1.73
R² = 0.98

ΔH_{H^-} experimental (kcal/mol)
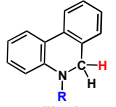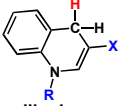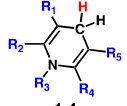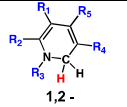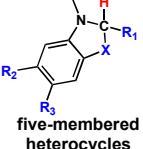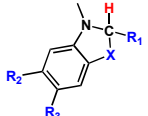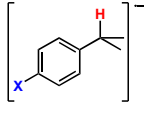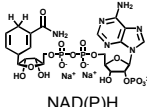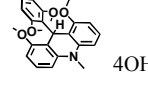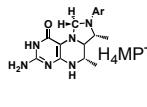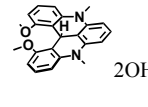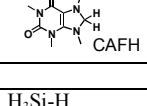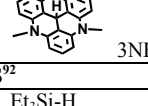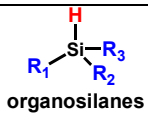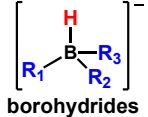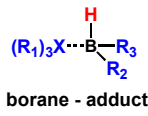
Figure 2. Calculated versus experimental hydricities: (a) free energy and (b) enthalpic hydricities in DMSO and MeCN. Data is reported in Table 2. Some computationally obtained hydricities are from references cited in Table 2. The rest have been calculated using Muckerman's scaling approach at the B3LYP/6-311++G(d,p)/CPCM level of theory.[98, 121-125] The 45° red line represents perfect agreement between experiment and theory, with a slope of unity and a y-intercept at 0. The dashed line is the correlation between calculated and experimental hydricities. Both fits were determined to have insignificant deviations from experiment with 95% confidence using the paired-t test, as is appropriate for such statistical analyses.[126] A p-value of 0.76 is obtained for (a) and 0.14 for (b), indicating that the mean hypothesized difference between experimental and computational methods is 0. The confidence intervals are (-1.29, 0.94) for (a) and (-0.09, 0.61) for (b). The inclusion of 0 in both intervals further supports the insignificance of the errors between the experimental and computational hydricities.
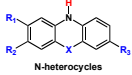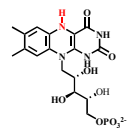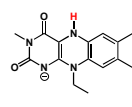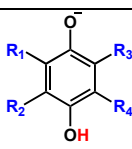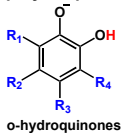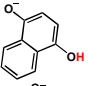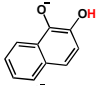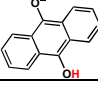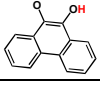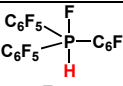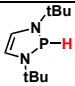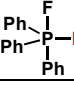
The experimental and computational methods described above provide thermodynamic and kinetic parameters for various metal-free hydrides (Table 2 and 3), which are exceptionally valuable for the evaluation of their structure-property relationships and applicability in catalysis. Sections IV and V provide an in-depth perspective regarding these parameters, including the structural and electronic factors that lead to stronger hydride donors, comparison with metal-based hydrides and applicability in stoichiometric and catalytic hydride transfer processes.

Table 2. A list of the experimental and calculated (in parentheses) values for ΔG_{H^-} (kcal/mol) and ΔH_{H^-} (kcal/mol) of the metal-free hydride donors reviewed here. Energies are for hydride transfers in acetoniotrile, unless otherwise noted. Hydridic hydrogens are shown in red.

STRUCTURE	#	COMPOUND	ΔG_{H^-}	ΔH_{H^-}	#	COMPOUND	ΔG_{H^-}	ΔH_{H^-}
			CARBON – BASED HYDRIDES					
benzyl-hydrides		*X = H, Ar =*						
	1	p-NO$_2$-Ph-	129[37] (127)[89]	-	8	p-Me-Ph-	112[37] (113)[89]	-
	2	m-CN-Ph-	129[37]	-	9	p-MeO-Ph-	107[37] (106)[89]	-
	3	p-CN-Ph-	122[37] (126)[89]	-		*X = CN, Ar =*		
	4	p-MeCO-Ph-	124[37]	-	10	p-CN-Ph-	129[39] (129)[89]	-
	5	p-F-Ph-	123[37] (118)[89]	-	11	Ph-	120[39] (122)[89]	-
	6	p-Cl-Ph-	123[37] (118)[89]	-	12	p-MeO-Ph-	106[39] (108)[89]	-
	7	Ph-	118[37] (118)[89] 113[39,b]	-				
triarylmethanes		*Ar$_1$ = Ar$_2$ = Ph, Ar$_3$ =*				*Ar$_1$ = Ar$_2$ = Ar$_3$ =*		
	13	H-	105[37] (104)[a,b]	(116)[a,b]	23	p-H-C$_6$F$_4$-	116[39,a]	-
	14	p-F-Ph-	98[39] (97)[b]	(104)[b]	24	p- Br-C$_6$F$_4$-	114[39,a]	-
	15	p-Ph-Ph-	96[37] (93)[a,b] 98[39]	(102)[a,b]	25	p-NO$_2$-Ph-	106[39,a]	-
	16	p-PhCO-Ph-	95[39] (97)[a,b]	(107)[b]	26	p-Cl-Ph-	98[37] (98)[a,b]	(108)[a,b]
	17	p-NO$_2$-Ph-	97[39] (98)[a,b]	(112)[b]	27	Ph-	99[39] (92)[92] 96[37] (94)[a,b]	(98)[92] (104)[a,b]
	18	p-Me-Ph-	96[39] (95)[b]	(101)[b]	28	p-Me-Ph-	93[39] (89)[b]	(97)[b]
	19	p-MeS-Ph-	95[39] (93)[b]	(98)[b]	29	p-MeO-Ph-	86[39] (83)[b]	(88)[b]
	20	m-MeO-Ph-	98[39] (97)[b]	(104)[b]	30	o,o-(MeO)$_2$-Ph- (6OH)	(86)[40] 84 (84)[40,a]	-
	21	p-MeO-Ph-	94[39] (91)[b]	(97)[b]	31	p-Me$_2$N-Ph-	74[39] (65)[b] 76[37,a]	(69)[b]
	22	p-Me$_2$N-Ph-	83[39] (81)[b]	(88)[b]				
fluorenes		*R =*						
	32	MeCO$_2$-	114[37] (113)[a,b]	(132)[a,b]	37	p-MeO-Ph-	101[39] (96)[a,b]	(106)[a,b]
	33	H-	109[37] (111)[a,b]	(127)[a,b]	38	Ph-	97[37] (101)[a,b]	(113)[a,b]
	34	t-Bu-	108[37] (105)[a,b]	(120)[a,b]	39	PhS-	97[37] (98)[a,b]	(109)[a,b]
	35	m-Cl-Ph-	102[37] (104)[a,b]	(116)[a,b]	40	MeO-	89[37] (90)[a,b]	(99)[a,b]
	36	Mes-	101[39] (101)[a,b]	(115)[a,b]	41	Me$_2$N-	70[39] (74)[a,b]	(80)[a,b]
dihydro- tricyclic heterocycles		*X = C-Me, R =*				*X = S, R =*		
	42	NO$_2$-	120[37,a]	-	50	Ph-	90[37] (86)[a,b]	(93)[a,b]
	43	Cl-	105[37,a]	-	51	H-	(90)[b]	94(93)[b]
	44	H-	98[37,a]	-		*X = O, R =*		
	45	Me-	95[37,a]	-	52	CN-	92[39] (94)[a,b]	(104)[a,b]
	46	MeO-	91[37,a]	-	53	H-	90[37] (87)[a,b]	(95)[a,b]
		R = H, X =			54	Ph-	89[37] (85)[a,b]	(92)[a,b]
	47	C-CH$_2$OPh	111[37,a]	-	55	p-MeO-PH-	87[39] (83)[a,b]	(90)[a,b]
	48	C-CH$_2$SPh	109[37,a]	-		*X = N-Me, R =*		
	49	C-CH$_2$OMe	102[37,a]	-	56	Ph-	76[85] (75)[85] 74[40] (73)[40,a]	-
					57	Me$_2$N-Ph-	70[40] (70)[40,a]	-
					58	H-	70[56] (72)[b]	81[72] (79)[b]
dihydro- phenanthridines		*R=*						
	59	p-CN-Bz-	66.4[60]	-	62	Me-	61.4[60]	-
	60	p-CF$_3$-Bz-	65.6[60]	-	63	H- (PheH$_2$)	(65.9)[b]	-
	61	Bz-	64.8[60]	-				

dihydroquinolines (structure)

		R = CH₂Ph, X =				R = Me, X =		
64	CN-	71.7[60] (77.2)[b]	83.9[88] (83.2)[b]		67	CN-	69.8[60] (76.3)[b]	81.1[88] (80.5)[b]
65	NH₂CO-	66.3[60] (71.4)[b]	75.8[46] (75.4)[b]		68	NH₂CO-	65.4[58]	-
66	H-	-	(70.1)[88]					

1,4-dihydropyridines (structure)

	R_1 = CN, R_2 = R_4 = R_5 = H, R_3 =				R_1 = CHO, R_2 = R_4 = R_5 = H, R_3 =		
69	p-CN-Bz-	(71.2)[b]	73.9[46] (75.4)[b]	75	p-CN-Bz-	(68)[b]	72.6[46] (71.2)[b]
70	p-Cl-Bz-	(70.4)[b]	72.4[46] (73.9)[b]	76	p-F-Bz-	(65.9)[b]	70.6[46] (69.3)[b]
71	p-F-Bz-	(69.7)[b]	71.4[46] (72.8)[b]	77	Bz-	(64.6)[b]	70.5[46] (67.9)[b]
72	Bz-	63[56](69.1)[b]	71.6[46] (73)[b]	78	p-Me-Bz-	(64.9)[b]	70.1[46] (68.5)[b]
73	p-Me-Bz-	(69)[b]	70.6[46] (72.5)[b]	79	p-MeO-Bz-	(65)[b]	69.7[46] (67.9)[b]
74	p-MeO-Bz-	(68.6)[b]	70.2[46] (71.9)[b]				

	$R1$ = COMe, R_2 = R_4 = R_5 = H, R_3 =				$R1$ = COOMe, R_2 = R_4 = R_5 = H, R_3 =		
80	p-CN-Bz-	(65.3)[b]	69[46] (68.9)[b]	86	p-CN-Bz-	(65)[b]	67.9[46] (69.1)[b]
81	p-Cl-Bz-	(63.9)[b]	67.6[46] (67.5)[b]	87	p-Cl-Bz-	(63.5)[b]	66.6[46] (67.6)[b]
82	p-F-Bz-	60.7[60] (63.6)[b]	67.2 [46] (67)[b]	88	p-F-Bz-	59.6[60](64.3)[b]	65.9[46] (67.3)[b]
83	Bz-	60[56] (62.9)[b]	67.1[46] (66.8)[b]	89	Bz-	59.5[60](63.3)[b]	65.8[46] (66.9)[b]
84	p-Me-Bz-	(63.2)[b]	66.5[46] (66.1)[b]	90	p-Me-Bz-	(62.8)[b]	65.2[46] (66.3)[b]
85	p-MeO-Bz-	(62.7)[b]	66.2[46] (65.7)[b]	91	p-MeO-Bz-	(63.3)[b]	64.9[46] (66.4)[b]

	R_1 = R_5 = COOEt, R_2 = R_4 = Me, R_3 =				$R1$ = CONH₂, R_2 = R_4 = H, R_3 = CH₂-Ph, R_5 =		
92	Me- (MeHEH)	61.5[40] (56)[b]	70 (65.7)[b]	94	-Br	(70)	68.2[46] (73.5)
93	H- (HEH)	(64.5)[b]	69 (70.4)[b]	95	-Me	(61.7)	61.5[46] (65.1)

	R_1 = CONH₂, R_2 = R_4 = R_5 = H, R_3 =						
96	p-CF₃-Ph-	(68)[b]	72.6[72] (72.6)[b]	104	p-CN-Bz-	(65)[b]	66.3[46] (67.9)[b]
97	p-Br-Ph-	(66)[b]	70.4[72] (70.4)[b]	105	p-Cl-Bz-	(63.6)[b]	65[46] (66.4)[b]
98	p-Cl-Ph-	(66.1)[b]	70.2[72] (70.5)[b]	106	p-F-Bz-	57[60] (62.7)[b]	64.3[46] (65.3)[b]
99	Ph- (PNAH)	(64.6)[b]	68.8[72] (68.9)[b]	107	Bz- (BNAH)	59[56] (62.6)[b]	64.2[46] (65.6)[b]
100	p-Me-Ph-	(63.9)[b]	67.5[72] (68)[b]	108	p-Me-Bz-	(62)[b]	63.6[46] (64.3)[b]
101	p-MeO-Ph-	(63.7)[b]	66.9[72] (67.2)[b]	109	p-MeO-Bz-	(62.5)[b]	63.1[46] (64.7)[b]
102	Et-	(60.8)[b]	61.5[46] (63.8)[b]	110	iPr	(60.6)[b]	61.3[46] (63.2)[b]
103	nBu-	(61.2)[b]	61.4[46] (63.8)[b]	111	nPr	(60.8)[b]	60.8[46] (63.8)[b]
				112	Me-	(61.9)[b]	60.7[46] (64.4)[b]

	R_2 = R_4 = R_5 = H, R_3 = Ph-CH₂, R_1 =		
113	-COOH	(65.4)[b]	67.5[46] (68.9)[b]
114	-CONHPh	(62.6)[b]	65.9[46] (66)[b]
115	-CONHEt	(60.9)[b]	63.8[46] (63.8)[b]
116	-H	(50.7)[b]	53[46](52.6)[b]
117	-Me	43[24] (49.4)[b]	48[46] (51.8)[b]

1,2-dihydropyridines (structure)

	R_4 = CONH₂, R_1 = R_2 = R_5 = H, R_3 =						
118	p-Cl-Ph-	(61.3)[b]	71.3[76] (67.9)[b]	124	p-MeO-Ph-	(61.9)[b]	66.8[76] (65.6)[b]
119	p-Br-Ph-	(60.9)[b]	70.9[76] (68)[b]				
120	Ph-	(62.7)[b]	69.5[76] (67.3)[b]		R_1 = R_2 = R_4 = R_5 = H, R_3 =		
123	p-Me-Ph-	(61.9)[b]	67.9[76] (66.3)[b]	125	H- (1,2-PyrH₂)	(41.5)[111]	-

five-membered heterocycles (structure)

	X = S, R_2 = R_3 = H, R_1 =				X = O, R_2 = R_3 = H, R_1 =		
126	m-Cl-Ph-	(69.9)[b]	76.9[47] (74.7)[b]	135	p-Cl-Ph-	-	93.4[47]
127	p-Br-Ph-	(69.7)[b]	75.7[47] (74.5)[b]	136	p-Br-Ph-	-	93.2[47]
128	p-Cl-Ph-	(69.3)[b]	75.6[47] (74)[b]	137	Ph-	-	91.2[47]
129	m-MeO-Ph-	(67.1)[b]	74.4[47] (71.4)[b]	138	p-Me-Ph-	-	89.3[47]
130	p-F-Ph-	(68.8)[b]	73.7[47] (73.6)[b]	139	p-MeO-Ph-	-	88.3[47]
131	Ph-	(68)[b]	73[47] (72.6)[b]		X = N-Me, R_1 = Ph, R_2 = H, R_3 =		
132	m-Me-Ph-	(66.4)[b]	72.1[47] (72.7)[b]	140	CF₃-	(55.7)[b]	61.9[47] (58.9)[b]
133	p-Me-Ph-	(67.2)[b]	71[47] (71.5)[b]	141	Cl-	(52.3)[b]	58.2[47] (56)[b]
134	p-MeO-Ph-	(66.3)[b]	69.9[47] (70.6)[b]	142	Me-	(48.2)[b]	51[47] (51.6)[b]
				143	MeO-	(48.9)[b]	49.7[47] (52.1)[b]

	X = N-Me, R_2 = R_3 = H, R_1 =						
144	p-NO₂-Ph-	(53.3)[b]	57.1[47] (57.3)[b]	158	p-MeO-m-Br-Ph-	(49.7)[b]	54.6[47] (53.2)[b]
145	m-NO₂-Ph-	(53.5)[b]	56.9[47] (57.2)[b]	159	Ph-	50[40] (49)[b]	54.1[47] (52.8)[b]
146	p-CN-Ph-	(52.6)[b]	56.7[47] (56.4)[b]	160	p,m,m-MeO₃-Ph-	(50)[b]	54[47] (52.8)[b]
147	p-Cl-m-Cl-Ph-	(52.6)[b]	56.6[47] (56.1)[b]	161	m-Me-Ph-	(47.1)[b]	53.8[47] (52.8)[b]
148	p-CF₃-Ph-	(51.8)[b]	56.5[47] (55.6)[b]	162	o-HO-Ph-	(47.5)[b]	53.8[47] (50.4)[b]
149	p-Cl-m-F-Ph-	(52.1)[b]	56.4[47] (56)[b]	163	p-MeO-m-MeO-	(48.9)[b]	53.5[47] (51.9)[b]

five-membered heterocycles

No.	R	value	value	No.	R	value	value
150	p-F-m-Br-Ph-	(50.8)[b]	56[47] (55.6)[b]		Ph-		
151	pMeO-mNO2-Ph-	(52.4)[b]	55.9[47] (55.7)[b]	164	p-Me-Ph-	(49.2)[b]	53.4[47] (51.9)[b]
152	m-Br-Ph-	(49.8)[b]	55.7[47] (54.8)[b]	165	o-Cl-Ph-	(50.5)[b]	53.2[47] (52.5)[b]
153	p-F-m-F-Ph-	(52.1)[b]	55.7[47] (55.8)[b]	166	p-Me-m-Me-Ph-	(48.3)[b]	53.1[47] (51.4)[b]
154	m-Cl-Ph-	(51.3)[b]	55.6[47] (56)[b]	167	p-MeO-Ph-	(48.5)[b]	52.9[47] (51.5)[b]
155	p-Br-Ph-	(50.4)[b]	55.2[47] (54.2)[b]	168	p-HO-Ph-	(48.9)[b]	52.6[47] (51.8)[b]
156	p-Cl-Ph-	(50.6)[b]	55.2[47] (54.2)[b]	169	o-Me-Ph-	(46.3)[b]	51.4[47] (50)[b]
157	m-MeO-Ph-	(49)[b]	54.6[47] (52.6)[b]	170	p-Me2N-Ph-	(44.9)[b]	50.6[47] (49.2)[b]
				171	H-	45[56] (47)[b]	49.5[47] (49.4)[b]
$X = N\text{-}Me$, $R_1 = Ph$, $R_2 = R_3 =$							
172	Me-	-	49[47]				

Radical-anion hydrides

No.	X	value	value	No.	X	value	value
$X =$							
172	NO2-	72[22] (79.3)[b]	(86.1)[b]	176	F-	32[22] (25.1)[b]	(23.7)[b]
173	MeCO-	50[22] (51.6)[b]	(55)[b]	177	H-	22[22] (18.3)[b]	(17.3)[b]
174	CN-	43[22] (43.8)[b]	(46.5)[b]	178	Me-	19[22] (16.5)[b]	(16.6)[b]
175	Cl-	37[22]	(25.7)[b]	179	MeO-	19[22] (18.2)[b]	(16.6)[b]
$X =$							
180	NO2-	70[22]	-	185	Cl-	52[22]	-
181	CHO-	63[22]	-	186	Ph-	50[22]	-
182	PhCO-	62[22]	-	187	H-	48[22]	-
183	CN-	59[22]	-	188	Me-	48[22]	-
184	PhS-	54[22]	-	189	MeO-	48[22]	-

selected hydride donors

No.		value	value	No.		value	value
190	NAD(P)H	-	(77.1)[88]	193	4OH	70.2 (73.2)[40, a]	-
191	H4MPT	(50)[92]	(58)[92]	194	2OH	58.2 (61.1)[40, a] 60.3 (62.9)[40]	-
192	CAFH	(53.2)[40]	57.6[48]	195	3NH	49.2 (48.7)[40] (46.9)[40, a]	-

SILICON – BASED HYDRIDES[92]

organosilanes

No.	R	value	value	No.	R	value	value
196	H3Si-H	(109)	(117)	201	Et3Si-H	(85.9)	(93.5)
197	Me2ClSi-H	(98.2)	(106)	202	Me2PhSi-H	(84.7)	(92.2)
198	PhH2Si-H	(96.3)	(105)	203	(iPr)3Si-H	(84.2)	(94.2)
199	Ph2HSi-H	(91.6)	(98.3)	204	(C6Me5)3Si-H	(74.3)	(84.4)
200	Ph3Si-H	(84.9)	(93.3)				

BORON – BASED HYDRIDES[92]

borohydrides

No.	R	value	value	No.	R	value	value
205	(cateholate)BH	(159)	(167)	217	[(AcO)3BH]⁻	(48.8)	(57)
206	(pinacolate)BH	(129)	(137)	218	[(C6F5)Ph2BH]⁻	(44.9)	((51.7))
207	9-H-BBN	(99)	(107)	219	[Ph3BH]⁻	(35.7)	(42.2)
208	[H2(CN)BH]⁻	(67.6)	(75.3)	220	[9-H2-BBN]⁻	(32.8)	(41.4)
209	[Cl3BH]⁻	(66.2)	(73)	221	[H2B(catecholate)]⁻	(26.3)	(33.1)
210	[(C6F5)3BH]⁻	(65)	(71.2)	222	[Et3BH]⁻	26[57] (24.4)	(32.2)
211	[(C6F5)2ClBH]⁻	(64.7)	(71.2)	223	[Mes3BH]⁻	(22.2)	(25.6)
212	[(C6F5)2HBH]⁻	(61.5)	(67.2)	224	[(secBu)3BH]⁻	(20)	(28.6)
213	[(C6F5)2PhBH]⁻	(54.5)	(62.1)	225	[H2B(pinacolate)]⁻	(11.7)	(18.3)
214	[(C6F5)2MesBH]⁻	(50.9)	(59.5)	226	[(tBu-O)3BH]⁻	(0.62)	(9.2)
215	[H3BH]⁻	(50.4)	(58.2)				
216	[F3BH]⁻	(49.1)	(56.2)				

borane - adducts

No.	R	value	value	No.	R	value	value
227	Et3N→Cl2BH	(77.7)	(85.4)	232	Et3N→205[d]	(55.1)	(63.4)
228	2,6-lut→Cl2B-H	(73.2)	(81.9)	233	tBu3P→205[d]	(52.7)	(60.3)
229	NH3BH3	(73.1)	(82)	234	((iPr)2Ph)2NHC→207[d]	(47.7)	(56.7)
230	DABCO→205[d]	(60.2)	(67.5)	235	iPr2NHC→207[d]	(47)	(56)
231	NH3→205[d]	(59.6)	(67.6)	236	DABCO→206[d]	(42.1)	(50.8)

OTHER HYDRIDES (N, O, P, and Ge)

N-heterocycles

X = S, R₁ = R₃ = H, R₂ =					*X = S, R₂ = R₃ = H, R₁ =*			
237	Br-	-	112^{73}		245	Cl-	-	111^{73}
238	Cl-	-	111^{73}		246	Me-	-	108^{73}
239	H-	-	110^{73} $(108)^{88}$		247	MeO-	-	107^{73}
240	Me-	-	107^{73}		*X = S, R₁ = H, R₂ = R₃ =*			
241	MeO-	-	104^{73}		248	Br-	-	114^{73}
242	Me₂N-	$(83)^{b}$	95^{73} $(91)^{b}$		249	Cl-	-	113^{73}
R₁ = R₂ = R₃ = H, X =					250	Me-	-	105^{73}
243	O	-	108^{73} $(109)^{88}$		251	MeO-	$(90)^{b}$	99^{73} $(98)^{b}$
244	N-Me	-	91^{73} $(91)^{88}$		252	Me₂N-	$(72)^{b}$	84^{73} $(78)^{b}$

253	FMNH₂	-	$(76.9)^{88}$	254		$(58.4)^{c}$	-

p-hydroquinones

R₂ = R₃ = R₄ = H, R₁ =					*R₁ = R₂ = R₃ = R₄ =*			
255	CN-	$(84)^{90,a}$	-		259	CN-	$(113)^{90,a}$	-
256	Cl-	$(73)^{90,a}$	-		260	Cl-	83^{38} $(83)^{a,b}$	$(92)^{a,b}$
257	H-	$70^{38}(69)^{a,b}$	$(73)^{a,b}$		261	Me-	58^{38} $(55)^{a,b}$	$(57)^{a,b}$
258	Me-	$(67)^{90,a}$	-		262	*R₁ = R₂ = Cl, R₃ = R₄ =*		
						CN-	101^{38} $(99)^{a,b}$	$(112)^{a,b}$

o-hydroquinones

R₂ = R₃ = R₄ = H, R₁ =					*R₁ = R₂ = R₃ = R₄ =*			
263	CN-	$(93)^{90,a}$	-					
264	Cl-	$(86)^{90,a}$	-		267	CN-	$(124)^{90,a}$	-
265	H-	$64^{38}(82)^{a,b}$	$(91)^{a,b}$		271	Cl-	70^{38} $(94)^{90,a}$	-
266	Me-	$(80)^{90,a}$	-		272	Me-	$(74)^{90,a}$	-
273		$(61)^{90,a}$	-		274		$(71)^{90,a}$	-
275		$(47)^{90,a}$	-		276		$(62)^{90,a}$	-

other hydrides								
	277		$(78)^{92}$	$(84)^{92}$	278		$(52)^{c}$	-
	279		$(44)^{92}$	$(53)^{92}$	280	Ph₃Ge-H	$(80)^{92}$	$(86)^{92}$

[a] Values in DMSO solvent.
[b] Values calculated here using Muckerman's approach.[86]
[c] Values calculated here using Krylov's approach.[40]
[d] Y→X, X is entry number of borane

Table 3. Mayr's kinetic parameters (s_N and N) as defined in equation 2 and measured for different metal-free hydride donors in DCM, MeCN or DMSO solvents.

STRUCTURE	SOLVENT	s_N	N	STRUCTURE	SOLVENT	s_N	N
7	DCM	1.32	-4.47	201[19]	DCM	0.7	3.58
53[80]	DCM	0.97	0.64	202[19]	DCM	0.75	3.55
58[19]	DCM	0.9	5.54	203[127]	DCM	0.73	2.93
93[78]	DCM	0.9	9	Me₃Si-H[127]	DCM	0.73	3.15
99[78]	DCM	0.87	7.53	(TMS)₃Si-H[19]	DCM	0.79	3.61
100[78]	DCM	0.95	7.68	208[78]	DMSO	0.67	11.52
101[78]	DCM	0.92	8.11		DMSO	0.81 (Na⁺)	14.74
	DCM	0.82	8.67	215[78]	DMSO	0.77 (K⁺)	15.14
107[78]	MeCN	0.7	9.8		DMSO	0.79 (Bu₄N⁺)	14.94
	W/MeCN=9/1	0.66	11.35	217[78]	DMSO	0.76	14.54
144[81]	MeCN	0.71	8.36	Et₃N→BBrH₂[79]	DCM	0.75	7.49
148[81]	MeCN	0.71	8.74	2,6-lut→BH₃[79]	DCM	0.75	10.33
154[81]	MeCN	0.71	9.38	Et₃N→BH₃[79]	DCM	0.75	8.9
159[81]	MeCN	0.72	9.72	(2,6-iPr₂Ph)₂NHC-9-H-BH₃[82]	DCM	0.81	9.55
164[81]	MeCN	0.7	10.14	iPr₂NHC-9-H-BH₃[82]	DCM	0.71	11.88
167[81]	MeCN	0.72	10.01	pyr→BH₃[79]	DCM	0.75	10.01
197[127]	DCM	0.73	0.79	p-MeO-pyr→BH₃[79]	DCM	0.75	11.01
198[19]	DCM	0.71	0.06	p-Me₂N-pyr→BH3[79]	DCM	0.76	12.44
199[127]	DCM	0.73	1.52	280[83]	DCM	0.62	3.99
200[19]	DCM	0.72	2.65	(nBu)₃Ge-H[83]	DCM	0.73	5.92

IV. Structure-Property Relationships

The experimental and calculated hydricities tabulated in this review can be utilized to derive important structure-property relationships that affect the thermodynamic and kinetic reactivities of metal-free hydride donors. This section describes the structural parameters (such as the electronegativity of the atom directly bound to the hydridic H-atom, the type of molecular framework and the presence of electron-donating/withdrawing groups) that correlate with the hydricities of various metal-free hydrides.

The strongest metal-free hydride donors can be found among boron-based derivatives, where a thermodynamic hydricity value as low as 0.6 kcal/mol in MeCN has been calculated for (t-BuO)₃B-H⁻ (entry 226).[92] Due to the low electronegativity of the B atom, boron-based hydrides exhibit advantageous bond polarization to create hydrides as polarized $B^{\delta+}-H^{\delta-}$ bonds, which contributes favorably to their hydride donating abilities. Furthermore, the negative charge of boron-based hydride donors increases their tendency to release a hydride ion. These two factors likely explain the large differences between boron-based compounds and other metal-free

analogs, as is evident from the ΔG_{H^-} values in MeCN obtained in the following series: BPh_3H^- (entry 219, $\Delta G_{H^-} = 36$ kcal/mol) < $GePh_3H$ (entry 280, $\Delta G_{H^-} = 80$ kcal/mol) < $SiPh_3H$ (entry 200, $\Delta G_{H^-} = 85$ kcal/mol) < CPh_3H (entry 27, $\Delta G_{H^-} = 92$ kcal/mol).[92] The hydrides made of group IV (C, Si and Ge) and group V (N and P) elements are generally weaker than their group III (B) analogs. In the case of carbon and nitrogen-based hydride donors, the electronegativities of C and N tend to polarize the bond in a protic $X^{\delta-}-H^{\delta+}$ sense, which weakens their hydride donating abilities. Despite the protic nature of the active H-atom, appropriate design of the hydride's molecular framework and substituents can be utilized to derive group IV and V hydrides with a wide range of hydride donating abilities, as is evident from Table 2. It is thus not a surprise that the group IV (NADH) and group V ($FADH_2$) hydrides are common donors in enzymatic reduction reactions. In the following subsections we describe the structural and electronic effects that control the hydride donor abilities of metal-free hydrides, particularly those based on carbon, silicon, boron and nitrogen derivatives.

Carbon-based Hydride Donors. Carbon-based hydride donors (Scheme 3) can be grouped into two general classes of compounds: arylmethanes and dihydro-heterocycles (tricyclic, bicyclic, dihydropyridines and five-membered heterocycles). Arylmethanes are relatively weak hydride donors with thermodynamic hydricities in the $\Delta G_{H^-} = 75 - 130$ kcal/mol range (entries $1 - 31$, Table 2).[37, 39, 40, 89, 92] Their ΔG_{H^-} values decrease as R^+ is stabilized through positive charge delocalization. For example, an increase in the number of aromatic rings lowers the ΔG_{H^-} value, as exhibited by the following trend: $PhCH_3$ (entry 7, $\Delta G_{H^-} = 118$ kcal/mol in DMSO, Table 2), Ph_2CH_2 (entry 13, $\Delta G_{H^-} = 105$ kcal/mol in DMSO) and Ph_3CH (entry 27, ΔG_{H^-} exp = 96 kcal/mol in DMSO).[37] Similarly, the introduction of electron-donating groups lowers the ΔG_{H^-} values, as exemplified by the DMSO values for the $(p\text{-}X\text{-}Ph)_3CH$ series, which range from 106 kcal/mol for $X=NO_2$ (entry 25)[39] to 76 kcal/mol for $X=Me_2N$ (entry 31, Table 2).[37] Furthermore, the substituent effect is additive, as shown for successive additions of nitro-groups to triphenyl-methane (entries 17, 25, 27) which results in an increase of ΔG_{H^-} values from 96 kcal/mol to 106 kcal/mol in DMSO, whereas the values drop from 99 kcal/mol to 74 kcal/mol in MeCN when multiple dimethyl amino-groups are introduced (entries 22, 27 and 31).[37, 39]

Scheme 3. Carbon-based hydride donors: a) arylmethanes and b) dihydro-heterocycles.

a) Arylmethanes
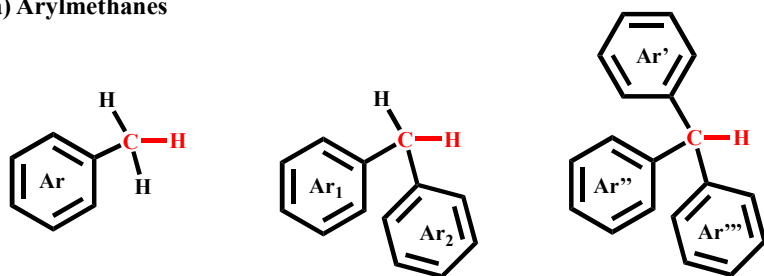
b) Dihydro-heterocycles
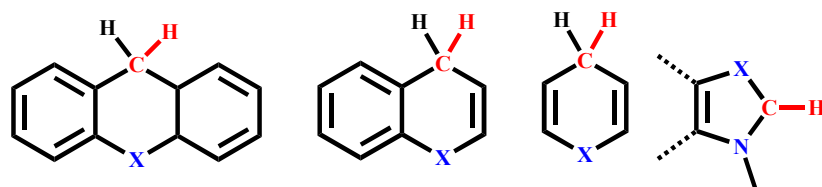
Generally, hydrides derived from heteroaromatic compounds are stronger donors than arylmethanes (ΔG_{H-} values range from 43 to 120 kcal/mol, Table 2), which is consistent with the stabilization of R^+ provided by aromatization. For example, the ΔG_{H-} of dihydroanthracene is lower than that of diphenyl methane by 7 kcal/mol (entries 44 and 13, Table 2).[37] The heteroatom plays a significant role in the stabilization of the R^+ cation product, with strongly electron-donating atoms (such as nitrogen) forming stronger hydride donors. For example, the hydrides derived from tricyclic heteroaromatics have thermodynamic hydricity values decreased in anthracene > xanthene > acridine series from 98 kcal/mol to 70 kcal/mol in MeCN (entries 44, 53 and 58).[37, 56] As the number of rings increases, two opposing factors control the stabilization of R^+: (i) larger heteroaromatic structures exhibit lower aromatic stabilization, which decreases the stabilization of R^+; (ii) the delocalization of the positive charge increases in larger, conjugated molecular frameworks, which increases the degree of R^+ stabilization. Which factor prevails depends on the particular system of interest. For instance, the aromatic stabilization energy prevails in the acridine < quinoline < pyridine series (entries 58, 65 and 107), where the ΔH_{H-} values decline from 81 kcal/mol to 64.2 kcal/mol in MeCN.[46, 72] On the other hand, the effect of extended charge delocalization dominates in the 4OH > 2OH > 3NH series (entries 193, 194 and 195) with ΔG_{H-} decreasing from 73.2 kcal/mol to 46.9 kcal/mol in MeCN.[40]

Dihydropyridines and imidazoles are two types of carbon-based hydrides that are direct analogs of biologically relevant cofactors: NAD(P)H[5] (entry 190) and methylene tetrahydromethanopterin[128] (H$_4$MPT, entry 191). The hydride-donating ability of NADH and other dihydropyridines is relatively high, where the aromatization of the forming pyridinium ring is the main driving force for the hydride transfer reaction. Furthermore, the positive charge is efficiently stabilized through the inductive effect of electron-donating groups, as shown for differently meta-substituted pyridines for which ΔH_{H^-} decreased from 71.6 kcal/mol to 48 kcal/mol in MeCN, in the following order: CN- > CHO- > COMe- > CO$_2$Me- > CONH$_2$- > H- > Me-, (entries 72, 77, 83, 89, 107, 116, and 117).[46] The imidazole-based compounds (H$_4$MPT and its analogs) are quite strong hydride donors, with ΔH_{H^-} values in the 49-57 kcal/mol range.[40, 47, 56] Besides the aromatization of the imidazolium cation product, the hydride donating abilities of benzimidazoles are additionally facilitated by the anomeric effect. Namely, the lone pairs of neighboring nitrogen atoms are in hyperconjugation with the antibonding orbital of C-H bond. The ability of the nitrogen to donate its electron pair is demonstrated in the thiazole < oxazole < imidazole series where ΔH_{H^-} ranges from 91.2 to 54.1 kcal/mol (entries 131, 137, and 159).[47]

Interestingly, the thermodynamic hydricity of carbon-based hydrides R-H can be significantly improved (by 40 - 90 kcal/mol) upon one electron reduction to form R-H$^{\cdot-}$ radical anions.[22] For example, radical anions of benzyl-hydrides exhibit very low ΔG_{H^-} values (as low as 19 kcal/mol, entries 178 and 179), making them the strongest carbon-based donors reported thus far. However, the potential applications of radical anion-based hydrides are limited by two drawbacks: (1) the potentials required for the hydride reduction are very negative ($E_{RH/RH^{\cdot-}} = -1$ to -3.24 V vs. NHE);[22] (2) the bond dissociation energies of radical anions are also quite low (35 – 50 kcal/mol), making them comparatively good hydrogen atom donors (see *ESI*).

Silicon-based Hydride Donors. Due to low electronegativity of the silicon atom, the Si-H bond is polarized favorably (as Si$^{\delta+}$–H$^{\delta-}$) for hydride ion donation and silanes tend to exhibit greater hydride donor ability than corresponding carbon-based analogs. This is exemplified in C-F activation by a silane, where critical fluoride abstraction is accompanied with the hydride transfer between silane and carbenium acceptor.[129] On the other hand, Si valence electrons reside in 3sp^3 orbitals, which do not overlap effectively with the neighboring C 2p orbitals to form pi-

bonds, as is the case for carbon-based hydrides. This effect is reflected in the similar thermodynamic hydricities calculated for Ph_3SiH (entry 200, ΔG_{H-} = 84.9 kcal/mol) and Et_3SiH (entry 201, ΔG_{H-} = 85.9 kcal/mol),[92] illustrating that the aromatic benzene rings do not contribute significantly to the stabilization of silylium cations formed upon the hydride transfer. This behavior is in stark contrast to the large differences in thermodynamic hydricities of their carbon-based analogs, as exemplified by comparing Ph_3CH (entry 27, ΔG_{H-} = 92 kcal/mol) and Me_3CH (ΔG_{H-} = 98 kcal/mol).[92] Another difference between silicon- and carbon-based hydrides is that the silylium cations formed upon hydride transfer are much stronger Lewis acids than the corresponding carbocations. This Lewis acidity likely improves the reactivity of silicon-based hydrides, as exemplified by their wide use in stoichiometric reductions by facilitating concerted additions to double bonds.[14] However, it does make hydride donation from silicon-based hydrides irreversible. Specifically, silanes add to an X=Y double bond in a R_3Si-H + X=Y → H-X-Y-SiR_3 manner, while the carbon-based systems, which form weaker Lewis acids, likely react in the following fashion: R_3C-H + X=Y → H-X-Y$^-$ + CR_3^+. In general, the low stability of silylium cations hinders experimental efforts to determine the hydricities of this class of compounds. However, several stable silylium cations were recently reported, where the steric crowding effect was used to lower their reactivity.[130]

Boron-based Hydride Donors. Experimental ΔG_{H-} reports of borohydrides are rare: the potential-pK_a method cannot be utilized, because reduction potentials of boranes are usually outside the solvent electrochemical stability window or are chemically irreversible.[131, 132] Currently, Super hydride[TM] (Et_3B-H$^-$) is the only borohydride with an experimentally determined thermodynamic hydricity in MeCN (entry 222, ΔG_{H-} = 26 kcal/mol), which was obtained using the hydride transfer method with a rhodium-based complex, $Rh(dmpe)_2H$, where dmpe is 1,2-bis(dimethylphosphino)ethane.[57] Thus, the insights into the factors that affect hydride donor ability of borohydrides have been obtained using computational data and kinetic measurements.[78, 79, 82, 92]

Hydride donor abilities of borohydrides can be tuned over a wide range: from ΔG_{H-} = 0.6 to 159.2 kcal/mol in MeCN (Table 2).[92] The stronger hydrides in this group, such as [(tBuO)$_3$BH]$^-$, [(secBu)$_3$BH]$^-$ and [Et_3BH]$^-$, match or even exceed the hydride donor abilities of the strongest

metal-based hydrides,[91] such as Rh(dmpe)$_2$H (ΔG_{H-} = 26.6 kcal/mol). The reasons for this are two-fold: (i) the low electronegativity and the small size of the boron atom polarizes the B-H bond towards hydride ion release and (ii) borohydrides are negatively charged, reducing the Coulombic attraction effect that must be overcome for hydride transfer. Overall, the hydride donor ability of borohydrides can be modified using electronic substituent effects. For instance, sodium borohydride has a thermodynamic hydricity of ΔG_{H-} = 50.4 kcal/mol (entry 215),[92] while replacing its hydrogen atoms with electron-donating groups decreases its ΔG_{H-} to 26 kcal/mol in Et$_3$B-H$^-$ (entry 222) and 0.6 kcal/mol in (tBu-O)$_3$B-H$^-$ (entry 226). Such behavior can be explained by an increase in the formal negative charge on the hydridic H-atom, as confirmed by extended Hückel theory.[133] Correspondingly, introduction of the electron-withdrawing cyano group leads to a weaker hydride, as exemplified by NaBH$_3$CN (entry 208, ΔG_{H-} = 68 kcal/mol). Similar effects have been observed in aryl-substituted borohydrides, where ΔG_{H-} values increased in the [Mes$_3$BH]$^-$ < [Ph$_3$BH]$^-$ < [(C$_6$F$_5$)$_3$BH]$^-$ series from 22 kcal/mol to 65 kcal/mol (entries 210, 219 and 223). In addition, ΔG_{H-} can be modulated using steric bulkiness. Specifically, the slightly improved thermodynamic hydricity of selectride ([secBu$_3$BH]$^-$, entry 224, ΔG_{H-} = 20 kcal/mol) over Super hydride^{TM} (entry 222, ΔG_{H-} = 24 kcal/mol) is a result of higher substituent crowdedness in the case of sec-Bu groups, which facilitates the loss of the hydride ion due to the release of the steric constraints. In terms of counter-cations, the similar nucleophilicity values in DMSO for NaBH$_4$ (N = 14.7), KBH$_4$ (N = 15.1) and Bu$_4$NBH$_4$ (N = 14.9) indicate that counter-ions are not involved during the critical hydride transfer step (Table 3).[78]

Trivalent boranes also act as hydride donors, albeit as much weaker hydrides than their corresponding anionic analogs.[79, 92] The trend can be observed when comparing 9-H-BBN (entry 207, ΔG_{H-} = 99 kcal/mol) with [9-H$_2$-BBN]$^-$ (entry 220, ΔG_{H-} = 33 kcal/mol).[92] Thermodynamic hydricities of trivalent boranes can be strengthened when coordinated to Lewis bases, as is evident when (catecholate)BH (entry 205, ΔG_{H-} = 159 kcal/mol) is coordinated to ammonia to form NH$_3$→(catecholate)B-H (entry 231, ΔG_{H-} = 60 kcal/mol).[92] The increase in hydricity depends on the basicity of the Lewis donor, as represented by the kinetic N-parameters in the following sequence of pyridine-borane adducts: pyridine→BH$_3$ (N = 10.0), p-MeO-pyridine→

BH$_3$ (N = 11.0) and p-Me$_2$N-pyridine→BH$_3$ (N = 12.4) (see Table 3).[79] However, the basicity is not the only effect that contributes to the reactivity since Et$_3$N→BH$_3$ (N = 8.9) has been shown to be a less reactive hydride donor than pyridine→BH$_3$ (N = 10.0) even though Et$_3$N is a stronger base than pyridine (pK_a(Et$_3$N) = 18.5 and pK_a(pyridine) = 12.5 in MeCN),[134] demonstrating that both steric and electronic effects have to be considered when tuning the reactivity of borohydrides.

Other Hydride Donors. Nitrogen- and oxygen-based hydrides are relatively weak, in accordance with the fact that N-H and O-H bonds are generally protic rather than hydridic. For example, nitrogen-containing tricyclic derivatives exhibit $\Delta H_{H\text-}$ values in the 90-110 kcal/mol range.[73] The enthalpic hydricity sensitively depends on the co-heteroatom present in the structural backbone: weaker donors within the group are phenothiazine derivatives (S as co-heteroatom, entry 239, $\Delta H_{H\text-}$ = 110 kcal/mol), followed by phenoxazine (O as co-heteroatom, entry 243, $\Delta H_{H\text-}$ = 108 kcal/mol) and phenazine (N as co-heteroatom, entry 244, $\Delta H_{H\text-}$ = 91 kcal/mol).[73] This heteroatom effect is due to different electron donating abilities of the heteroatom, with nitrogen being the most electron-donating heteroatom. Interestingly, one of the most abundant biological cofactors for hydride transfer processes is a nitrogen-based structure, even though N-based hydride donors are relatively weak. Namely, the reduced forms of flavin-adenine dinucleotide (FADH$_2$) and flavin mononucleotide (FMNH$_2$) serve as hydride donors in enzymatic reduction processes (Scheme 4a).[5] The thermodynamic hydricity of flavins in enzymatic reactions is often strengthened by deprotonation to FADH$^-$ or FMNH$^-$ anions. The effect of deprotonation on $\Delta G_{H\text-}$ can be observed by comparing $\Delta G_{H\text-}$ values for FMNH$_2$ (entry 253, 76.9 kcal/mol)[88] and the deprotonated model compound (entry 254, $\Delta G_{H\text-}$ = 58.4 kcal/mol).

Scheme 4. Representations of FAD and hydroquinone N-H (a) and O-H hydrides (b). Hydridic bonds are shown in red, whereas the negatively charged heteroatoms are shown in blue. The dashed lines of the hydroquinones represent a substitution or the presence of another phenyl ring.

a)

R = ADP (FADH$_2$) or P$_i$ (FMNH$_2$)   R = ADP (FADH$^-$) or P$_i$ (FMNH$^-$)

b)

p - hydroquinones   *o* - hydroquinones
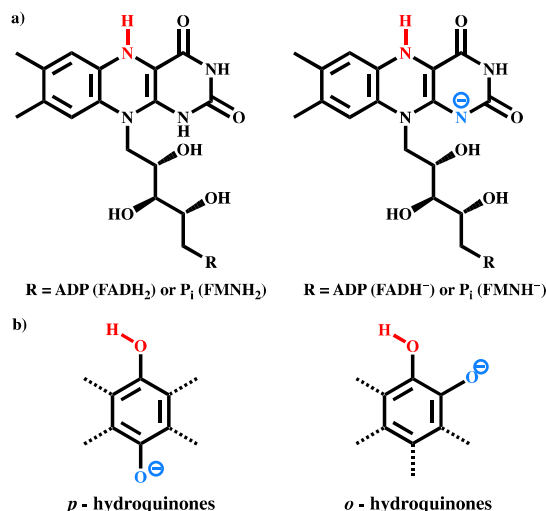
Among oxygen-based hydrides, deprotonated hydroquinones are weak to mild hydride donors.[38, 90] For instance, ortho-hydroquinone anion has a thermodynamic hydricity of $\Delta G_{H-} = 82$ kcal/mol (entry 265), while para-hydroquinone anion is a stronger hydride donor, with $\Delta G_{H-} = 69$ kcal/mol (entry 257) (Scheme 4b). The lower ΔG_{H-} of the *o*-isomer is caused by the stabilization of the hydride form due to the presence of the O-H---O hydrogen bond. In general, quinone-hydroquinone systems are better tuned for hydride abstraction rather than for hydride donation, because the aromaticity of hydroquinone is lost upon hydride release in contrast to the pyridine-based hydrides.[90] This effect can be observed by comparing the thermodynamic hydricities of hydroquinones with an expanding number of benzene rings: anthrahydroquinone > naphthahydroquinone > benzohydrophenone (entries 257, 273 and 275, Table 2). Thus, it is not surprising that this group of hydrides participates in electron transfer rather than hydride transfer processes.

Hydrides of other metal-free elements (phosphorus, germanium and tellurium) have not been widely used as hydride donors and therefore have not been examined in terms of their hydricities. Because of the large differences in atomic sizes (poor orbital overlap) and the electronegativities of these elements are similar to hydrogen ($\chi(P) = 2.19$, $\chi(Ge) = 2.01$ and $\chi(Te) = 2.10$), the bonds that these elements form with hydrogen are not sufficiently polarized for hydride transfer chemistry. However, the polarity of the X-H bond is tunable with substituents and reaction conditions. For example, Cl$_3$Ge-H acts as a proton donor, whereas Et$_3$Ge-H acts as a

hydride donor in reactions with ketones.[135] In terms of thermodynamic hydricity, phosphorus-based hydrides are promising hydride donor candidates, with calculated values comparable to BH_4^-.[92] Organogermanes exhibit hydride donor abilities similar to organosilanes (ΔG_{H^-} ~80 kcal/mol and N= 3-6).[19, 92]

ΔG_{H^-} vs. ΔH_{H^-}. Comparing the values obtained in ΔG_{H^-} and ΔH_{H^-} measurements indicates when entropic effects on hydride donation are significant. While experimental ΔH_{H^-} values are simply obtained through calorimetry, the methods for determining ΔG_{H^-} values are often challenging, as discussed in the Experimental Methods section. Consequently, significantly more ΔH_{H^-} values are reported in the literature than ΔG_{H^-} values, and it is often assumed that entropic contributions to the thermodynamic hydricity are negligible.[45-48, 72-76] To test the validity of this assumption, Figure 3 plots ΔH_{H^-} and ΔG_{H^-} values for the metal-free hydrides listed in Table 2. ΔS_{H^-} is positive for all hydrides, causing the room temperature ΔG_{H^-} values to be ~6 kcal/mol lower than their corresponding ΔH_{H^-} values. This relatively consistent offset suggests that ΔH_{H^-} values can be used to compare the relative hydride donor abilities of compounds within a family of hydrides. However, entropic contributions should not be neglected, especially considering the large variations for different groups of hydride donors: from $T\Delta S_{H^-}$ = 3.6 kcal/mol for dihydropyridines to 12.5 kcal/mol for fluorenes (at 298 K). Higher $T\Delta S_{H^-}$ values were found for larger molecules, possibly due to a larger entropic contribution from a solvent[56] or because hydride transfer significantly affected the low frequency skeletal modes of the larger molecules.
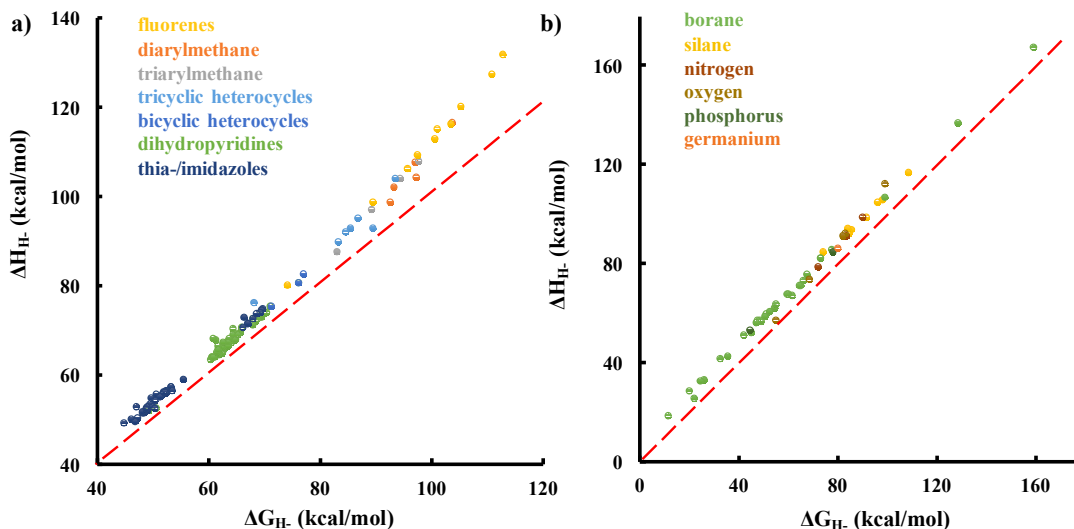
Figure 3. The comparison between ΔH_{H^-} and ΔG_{H^-} at 298 K for hydrides tabulated in Table 2 for: (a) carbon-based and (b) other hydride donors. The red dashed lines represent the condition $\Delta H_{H^-} = \Delta G_{H^-}$ at which $T\Delta S_H = 0$. The data all lie above this line, indicating that $\Delta H_{H^-} - \Delta G_{H^-} = T\Delta S_{H^-}$ is positive for metal-free hydride donors. The average $T\Delta S_{H^-}$ contributions for different classes of hydrides at room temperature are as follows: carbon- fluorenes (12 kcal/mol), diphenylmethanes (9 kcal/mol), triphenylmethanes (7 kcal/mol), tricyclic heterocycles (7 kcal/mol), bicyclic heterocycles (5 kcal/mol), dihydropyridines (4 kcal/mol) and five-membered (5 kcal/mol); boron- (8 kcal/mol), silicon- (8 kcal/mol), nitrogen- (7 kcal/mol), oxygen- (7 kcal/mol), phosphorus- (8 kcal/mol) and germanium-based donors (6 kcal/mol).

Kinetic Aspects of Hydride Transfers. Early experimental studies performed by Kreevoy reveal that hydride transfer rates scale linearly with the driving force for hydride transfer reactions between NADH-analogs.[58-60, 136] His experimental data was fit based on the quadratic dependence predicted by Marcus theory for non-adiabatic electron transfer,[137, 138] as shown in eq (7):

$$\Delta G^{\ddagger} = \frac{(\lambda + \Delta G_0)^2}{4\lambda} \qquad (7)$$

where λ is the reorganization energy associated with the electronic reorganization of the solute and configurational reorganization of the solvent, $\Delta G^{\ddagger}$ is the activation free energy, and ΔG_0 is the free energy of the hydride transfer reaction. However, the experimental results exhibit a linear rate dependence between the thermodynamic and kinetic parameters due to a large

difference between the reorganization energies and respective reaction free energies ($\lambda \sim 80$ kcal/mol $\gg \Delta G_0 = -10$ to 0 kcal/mol).

Warshel and coworkers[139, 140] provided a possible explanation for these experimental observations by modeling the adiabatic nature of S_N2 reactions (including hydride transfers) using a modified Marcus expression to calculate the activation free energy:

$$\Delta G^{\ddagger} = \frac{(\lambda + \Delta G_0)^2}{4\lambda} - H_{rp}(X^{\ddagger}) + \frac{H_{rp}^2(X_r^0)}{\lambda + \Delta G_0} \qquad (8)$$

Here, $H_{rp}(X^{\ddagger})$ and $H_{rp}(X_r^0)$ are electronic coupling matrix elements at the transition-state and reactant geometries, respectively. Computing these matrices allows for the determination of the non-adiabatic reaction surface, which can be traced by calculating the energies along the reaction coordinate while freezing the electron density of the surroundings. This assumes that the hydride transfer occurs at rates much faster than reorganization. The adiabatic model yielded a larger reorganization energy for NADH analogs ($\lambda = 236$ kcal/mol) than those obtained using the non-adiabatic approach, which is consistent with the fact that the electronic coupling terms are significant for hydride transfer processes.[139] Again, the larger reorganization energy (relative to the reaction free energy) further justifies the linear free energy relation for hydride donors observed in experiments.[58-60, 136]

Recent studies of hydride transfer utilize linear relationships between thermodynamic and kinetic (N) parameters to describe the reactivity of hydride donors.[93] Figure 4 shows a linear dependence between experimental N values and ΔG_{H^-} for structurally-related hydrides. Although only a few observations can be made due to the dearth of available data, some useful conclusions can be drawn about these linear relationships. Namely, the intercepts are correlated to the intrinsic activation energies (barriers) of the hydride transfer reactions.[141] The intrinsic barriers for borohydrides and silanes are lower than those of carbon-based hydrides, possibly due to the role of their conjugate acceptors, which have higher Lewis acidities, in stabilizing the hydride transfer products. Furthermore, the slopes of the linear correlations represent the sensitivity of the kinetics to structural changes within each hydride donor class.[81] Smaller slopes in the cases

of borohydrides and silanes indicate that their nucleophilicity values are only slightly enhanced by the larger thermodynamic driving force (lower $\Delta G_{H\text{-}}$) of a hydride donor. In contrast, carbon-based hydrides have steeper slopes, indicating that changes in their thermodynamic hydricities considerably alter the rates of hydride transfer.
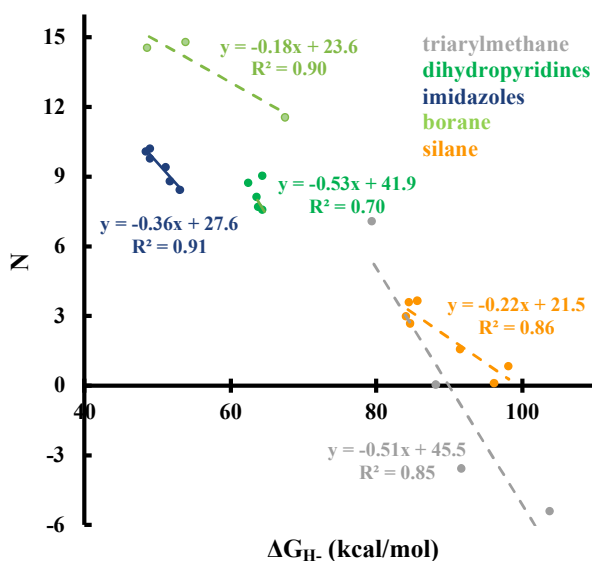

Figure 4. Linear free energy relations expressed with respect to the kinetic nucleophilicity parameter N and the thermodynamic hydricity (in kcal/mol) for boranes, silanes, and other subgroups of carbon-based hydrides. N values for borohydrides are measured in DMSO, while all other values are obtained in dichloromethane. Caution must be exercised when comparing N values because boranes are reported in a more polar solvent relative to others. All $\Delta G_{H\text{-}}$ values are reported in MeCN.

Solvation Effects. Solvation plays a major role in determining the strength of a hydride donor, as demonstrated by $\Delta G_{H\text{-}}$ values in different solvents as shown in Table 2. Most hydrides tend to be stronger (possess a lower $\Delta G_{H\text{-}}$ value) in more polar solvents, which can be attributed to more effective charge stabilization by the solvent molecules solvating the hydride ion. Most of the experimentally determined thermodynamic hydricities of metal-free species were obtained from measurements in MeCN and DMSO solvents, which have dielectric constants (ε) of 37.5 and 46.7, respectively. The results show that $\Delta G_{H\text{-}}$ are ~2 kcal/mol lower in DMSO relative to their values in the less polar solvent MeCN. While aqueous $\Delta G_{H\text{-}}$ values have not been evaluated for

metal-free hydrides, transition metal hydrides are shown to be stronger in water ($\varepsilon = 80$) by at least 20 kcal/mol relative to their ΔG_{H^-} values in MeCN.[1, 62, 142] Similar effects are also observed for nucleophilicity. Hydrides exhibit larger nucleophilicities in more polar solvents, as exemplified by 1-benzyl-1,4-dihydronicotinamide (entry 107, Table 3) when measured in DCM ($N = 8.7$), MeCN ($N = 9.8$), and a 9:1 water/MeCN mixture ($N = 11.4$).[78]
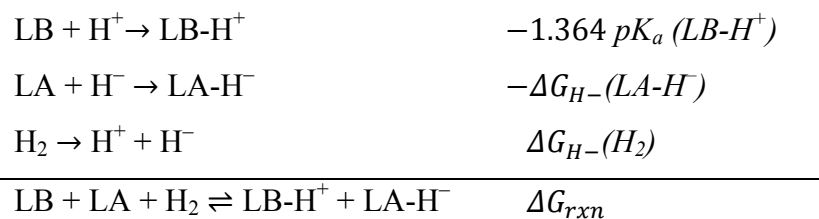

V. Relevance to Catalysis

To efficiently utilize hydrides in catalytic reduction reactions, one needs to strike a balance between the hydride donating ability of R-H and the energy required to regenerate it from R^+ to close the catalytic cycle. While the catalytic behavior of metal-based hydrides has been reported for many reduction reactions,[2, 3, 143] metal-free hydrides often behave only as stoichiometric reducing reagents rather than catalysts. This section describes the challenges associated with the use of metal-free hydrides in catalysis and outlines possible approaches to improve their performance. Two specific types of catalytic processes are considered: (i) hydrogen activation catalysis,[9, 10, 67, 69, 144-149] which became a very active area of research after the discovery that frustrated Lewis pairs heterolytically dissociate H_2 and (ii) electrocatalytic reduction processes,[150-153] particularly those relevant to solar fuels.

Catalytic Hydrogen Activation. Molecular hydrogen is an inert molecule whose activation requires a catalyst which can perturb the electron density of the H-H bond. Transition metal centers successfully achieve H-H bond polarization using occupied d-orbitals as proton acceptors (Lewis bases) and unoccupied d-orbitals as hydride acceptors (Lewis acids).[3] Among metal-free systems, analogous chemistry has been observed for carbenes, but they were not widely applied to catalysis due to challenges associated with the closure of the catalytic cycle, for example, the low reactivity of the H_2-adduct.[154] The breakthrough in the field of metal-free H_2 activation was made by Stephan, who showed that H_2 could be heterolytically cleaved using frustrated Lewis acid/base pairs (FLPs).[155] Since this initial discovery, a number of FLPs have been applied to various catalytic reductions of different C=C, C=N and C=O substrates using boranes, silyliums

and carbocations as Lewis acids (LA) and amines, phosphines and carbenes as Lewis bases (LB).[9, 10]

The applicability of FLPs to catalytic reactions is determined by the ability of the tandem pair to reversibly activate normally inert hydrogen. Thermodynamic driving forces for the relevant catalytic steps, that is H_2 dissociation and subsequent reduction of substrates by the hydride, can be readily determined from the thermodynamic hydricities and pK_a values of the relevant species, as shown in Scheme 5.[156] Namely, the free energy of H_2 activation by FLPs (ΔG_{rxn}) can be expressed using a thermochemical cycle consisting of the hydride affinity of the Lewis acid ($-\Delta G_{H-}(LA\text{-}H^-)$) and the basicity of the Lewis base ($-1.364\ pK_a(LB\text{-}H^+)$). While these parameters describe the hydride and proton transfer abilitis of the hydride and protonated Lewis base, the sum also indicates the applicability of FLPs in catalysis. For example, $\Delta G_{H-}(H_2)$ is 76 kcal/mol in MeCN,[41] indicating that reversible activation will occur when the relationship $1.364\ pK_a(LB\text{-}H^+) + \Delta G_{H-}(LA\text{-}H^-) \sim 76$ kcal/mol is satisfied. This sets a limit for the hydride strength of intermediate LA-H$^-$ donors, which determines the spectrum of reduction reactions that are feasible. If substrates require a strong hydride donor for their reduction, then stronger Lewis bases are required to satisfy the reversibility requirement. Investigations of a diverse set of LA and LB pairs have been reported in the literature.[9, 10, 67, 69] In most cases where catalysis was observed, bases with $pK_a = 7 - 18$ in MeCN are used, whereas LA thermodynamic hydricities range between 50 to 70 kcal/mol, indicating that ΔG_{rxn} varies from -10 to 5 kcal/mol.[144-149] The Selected Applications section describes some specific examples in more detail, along with the associated thermodynamic parameters.

Scheme 5. Reaction steps for dihydrogen activation by Frustrated Lewis Pairs.

LB + H$^+$ → LB-H$^+$	$-1.364\ pK_a\ (LB\text{-}H^+)$
LA + H$^-$ → LA-H$^-$	$-\Delta G_{H-}(LA\text{-}H^-)$
H$_2$ → H$^+$ + H$^-$	$\Delta G_{H-}(H_2)$
LB + LA + H$_2$ ⇌ LB-H$^+$ + LA-H$^-$	ΔG_{rxn}

Electrocatalytic Reductions. Different thermodynamic arguments are considered for catalysis in which the recovery of the active hydride form is achieved using electrochemical or

photochemical methods. These approaches are particularly relevant to energy storage applications, where the ability of a hydride donor to form fuels, such as H_2 and CH_3OH, is defined by the thermodynamic hydricity of the fuel. For example, the ΔG_{H^-} values of H_2 and formate (the first intermediate in CO_2 reduction) in acetonitrile are 76 kcal/mol and 44 kcal/mol, respectively.[41, 157] Competent hydride donors should have thermodynamic hydricities slightly below these limits in order to provide a finite driving force to make the thermodynamics of hydride transfer favorable. While having larger driving forces for hydride transfer seems desirable, larger driving forces are accompanied by higher overpotentials to drive recovery of the catalyst. Figure 5 and Table 2 show that most metal-free donors are sufficiently strong hydrides to reduce protons, but only relatively strong hydride donors can serve as reductants for CO_2. However, successful CO_2 reduction could be performed using weaker hydride donors, if the hydride transfer is accompanied by a proton transfer ($\Delta G(CO_2/HCOOH)$ = 72 kcal/mol in MeCN, see *ESI*).

For an ideal catalyst, electrochemical closure of the catalytic cycle should be achieved at a potential that is equal to the standard reduction potential for the fuel forming reactions (0.46 V vs. NHE for H^+/H_2 and -0.23 V vs. NHE for $CO_2/HCOO^-$, see *ESI*). Thus, evaluation of ΔG_{H-} values of hydride donors R-H and E_1 values of the conjugate hydride acceptors provides insight into metal-free hydride donors that should be screened for the target reduction process. Figure 5 compares these parameters for both metal-free and metal-based hydride donors,[26-29, 31, 32, 34, 36, 37, 40, 41, 65, 158] including those relevant to fuel-forming proton and CO_2 reduction processes. Interestingly, a scaling relationship is observed between the first reduction potential E_1 of the oxidized form (Scheme 2) and the ΔG_{H-} values across different metal-free hydride donor groups. The existence of this scaling relationship reflects the fact that bond dissociation energies (BDEs) of hydride donors are relatively similar to each other and that the intercept of the plot is directly related to these values (see ESI for more information). Most metal-free hydride donors have BDE values of approximately 75 kcal/mol (Figure S2 in *ESI*), giving rise to the observed linearity. BDE values for the metal-based hydrides obtained from the correlation were found to be lower (~60 kcal/mol), which explains their higher activity.
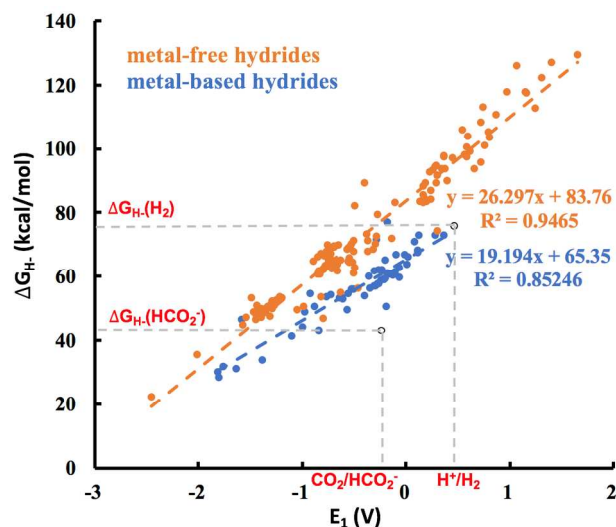
Figure 5. The scaling relationships between the thermodynamic hydricity ΔG_{H-} and the first electron reduction potential E_1 of the oxidized form for metal-free (orange) and metal-based hydrides (blue). The ΔG_{H-} value for dihydrogen $\Delta G_{H-}(H_2) = 76$ kcal/mol and carbon dioxide $\Delta G_{H-}(CO_2) = 44$ kcal/mol along with reduction potentials $E(H^+/H_2) = 0.46$ V and $E(CO_2/HCO_2-) = -0.23$ V (both vs. NHE) are presented as black circles. The dashed gray line helps to estimate the overpotential.

The scaling relationship between E_1 and the thermodynamic hydricity has important consequences for the catalyst performance of the hydride donor. For example, it implies that the lowest possible overpotential that can be achieved for proton reduction using metal-free hydride donors is 0.3 V, while metal-based systems can operate at essentially zero overpotential. In the case of CO_2 reduction, both metal-free and metal-based systems contain sizeable overpotentials, ranging from 1.5 to 1.1 V (Figure 5). However, this overpotential is likely lower if CO_2 is reduced by a proton-coupled hydride transfer where the coupled proton transfer stabilizes the preceding hydride transfer.

The analysis shown in Figure 5 only considers E_1 values and thus fails to address the fact that recovery of the hydride catalysts requires two electron transfers. The potentials required for the second electron reduction E_2 (Scheme 2) tend to be more energetically demanding, often requiring more than 1 V energy input in addition to E_1. In contrast, the second electron reduction of metal-based analogs is less demanding, where differences between two potentials ($\Delta E = E_1 - E_2$)

are ~0.5 V (Figure 6a).[26-29, 31, 32, 34, 36, 37, 40, 41, 65, 158] The ability of metal complexes to screen the second incoming charge is possibly due to large structural changes that occur upon the first electron reduction.[65, 159] To illustrate the difference between the energy requirements for closure of the catalytic cycle, Figure 6b compares the well-known Dubois Ni-complex catalyst[160, 161] with a metal-free hydride donor of similar ΔG_{H^-} (2OH).[40] While the first electron transfers occur at comparable reduction potentials (–0.4 V vs. NHE for the Ni-complex and –0.5 V vs. NHE for 2OH), there is a significant difference in the second reduction potentials (–0.5 V vs. NHE for Ni-complex and –1.4 V vs. NHE for 2OH).[40, 160]
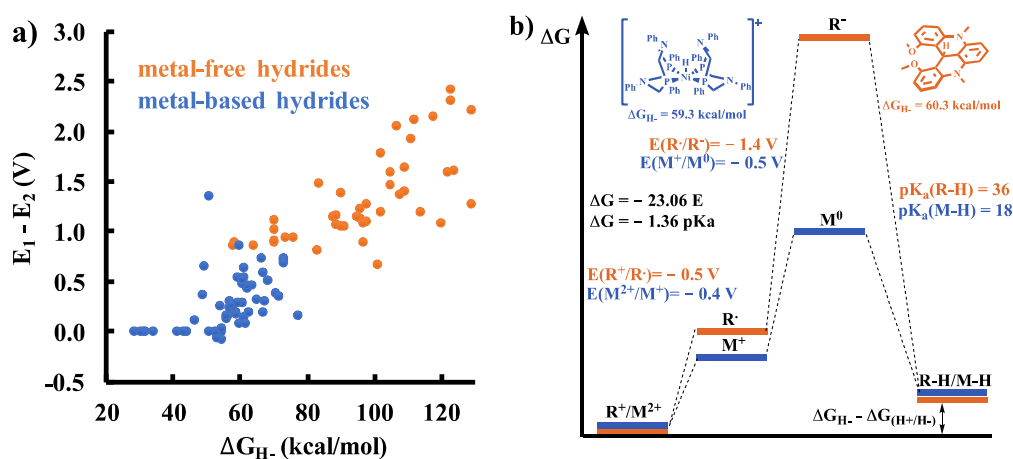

Figure 6. (a) The difference in the first and second reduction potentials (E_1-E_2) as a function of the thermodynamic hydricity (ΔG_{H^-}) for metal-free and metal-based hydrides. (b) The illustrative comparison of the energy profiles required for hydride catalyst recovery for metal-catalyst (Ni-complex) and for a metal-free hydride donor (2OH) possessing similar ΔG_{H^-}.

Very negative E_2 values of some metal-free hydrides are a likely reason why metal-free hydride donors are not often utilized in catalysis. These drawbacks of some metal-free models can be addressed by identifying approaches that enable catalyst recovery by lowering the reduction potentials without affecting their hydride donor ability. For example, the second reduction step can be achieved via a proton-coupled electron transfer mechanism, a tactic that is frequently used in many natural and artificial catalysts.[153, 162] Specifically, the reduced forms of natural flavin-based cofactors are regenerated using such proton-coupled reduction steps, as discussed in the Selected Applications section. Proton-coupled reduction is often utilized in metal-based catalysis

to achieve efficient recovery of the hydride form.[55] For example, a comparative study of the photochemical hydrogen evolution reaction by Fe, Co and Ni hydrides indicates that the Co-based photocatalyst performs much better than the Ni-based analog due to differences in the *pKa* values between $[Co^{III}\text{-H}]^{2+}$ (*pKa*=7) and $[Ni^{III}\text{-H}]^{2+}$ (*pKa*=-0.4).[163] An interesting approach, reported recently by Berben, involves the use of Al ion coordination to shift the reduction potentials of an imine-based ligand to less negative values.[164]

VI. Selected Applications

This section describes three applications of metal-free hydrides in catalysis. The first example involves natural photosynthesis, in which the pyridine-based NADPH cofactor is a key catalyst that stores electrons extracted from water in the photochemical event and transfers them to the Calvin cycle, where activated CO_2 is reduced. The second application describes artificial photosynthesis, where NADH analogs are utilized for the same purpose as the natural cofactors: to accumulate electrons photochemically and reduce CO_2 in a sequence of proton-coupled hydride transfer steps. The third example describes reduction of double bonds in various substrates using molecular hydrogen. Here, metal-free FLP catalysts serve to activate molecular hydrogen using a hydride/proton addition mechanism. The following text describes the key aspects of each catalytic system.

Natural Photosynthesis. The most abundant use of metal-free hydrides in catalysis is in natural photosynthesis, a large-scale process that uses CO_2 as a feedstock to convert and chemically store solar energy in energy-dense molecules. Nature chose NADPH to serve as the primary carrier of reducing power for the photosynthetic conversion of CO_2 into carbohydrates within the Calvin cycle.[5] The use of a hydride transfer process to reduce CO_2 avoids the generation of high-energy and unstable odd-electron reduced intermediates necessarily formed in sequential electron transfer processes. However, the direct reduction of CO_2 by enzymatic NADPH is likely thermodynamically unfavorable because the thermodynamic hydricity of the model NADH compound (entry 107, $\Delta G_{H-} = 59$ kcal/mol)[46] is significantly higher than that required for CO_2 reduction ($\Delta G_{H-}(HCO_2^-) = 44$ kcal/mol).[144] Consequently, in addition to the low solubility of CO_2 in aqueous media, photosynthetic organisms have evolved to first capture and activate CO_2

in the form of 1,3-diphosphoglycerate and then perform the reduction step using NADPH.[165] The enzyme that catalyzes the key hydride transfer step, glyceraldehyde 3-phosphate dehydrogenase, activates the C=O group by converting it into a thioester using cysteine, while the histidine residue serves as a proton source, as presented in Scheme 6a.[166]

Scheme 6. Illustration of the catalytic behavior of NADPH in photosynthetic organisms. (a) Reduction of 1,3-diphosphoglycerate via hydride transfer from NADPH in glyceraldehyde 3-phosphate dehydrogenase (Calvin cycle);[166] (b) Flavin-mediated regeneration of NADPH from NADP⁺ in ferredoxin NADP⁺ reductase (Photosystem I).[167, 168] Energetically favored routes represent proton-coupled electron transfer processes (shown in blue), or hydride transfer processes (shown in red). The grey route shows an unfavorable pathway for NADPH regeneration. The estimated hydride donor ability of NADP- and FAD- cofactors are approximated from corresponding model compounds (entries 107 and 254 in Table 2).
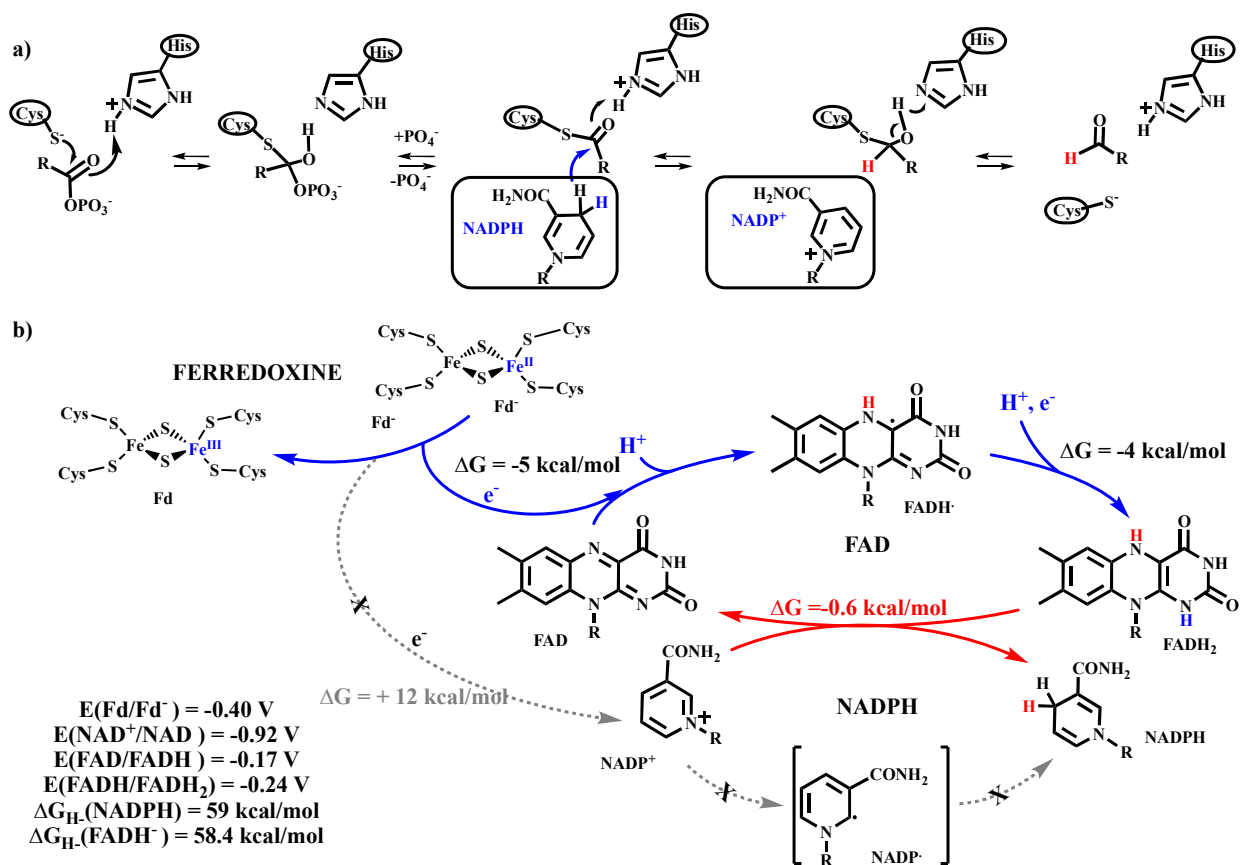
As discussed in the Relevance to Catalysis section, the recovery of metal-free hydrides is energetically challenging due to the very negative reduction potentials E_1 and E_2 associated with the reduction of the conjugate hydride acceptor. However, photosynthetic organisms utilize a powerful approach to regenerate NAPDH. The reduction of $NADP^+$ is driven by highly reducing electrons generated from water splitting, an uphill light-driven process.[5] Electron equivalents produced in the photochemical process are then supplied to ferredoxin-$NADP^+$ reductase to reduce $NADP^+$.[167, 168] The reductase contains an iron-sulfur cluster (ferredoxin), that channels electrons to the active site, and a FAD cofactor, which mediates between the one-electron donor ferrodoxin and the hydride acceptor $NADP^+$, as illustrated in Scheme 6b.

In the absence of flavin mediation, ferredoxin is not a sufficiently strong reducing agent to reduce $NADP^+$, consistent with the unfavorable thermodynamics of electron transfer expressed by the more negative reduction potential of the $NADP^+/NADP^.$ couple ($E = -0.92$ V vs. NHE) relative to ferrodoxin ($E = -0.43$ V vs. NHE).[169, 170] However, the flavin cofactor can undergo both one-electron reductions at moderately negative potentials because each step is coupled to a concerted proton transfer ($E(FAD/FADH^.) = -0.17$ V vs. NHE and $E(FADH^./FADH_2) = -0.24$ V vs. NHE).[162, 169] Thus, flavin serves as a mediator that accepts electrons from ferredoxin and subsequently delivers them to $NADP^+$ through a hydride transfer. The proton-coupled hydride transfer reduction mechanism observed for flavin cofactors is an approach that can be expanded to future artificial metal-free hydride donors to: i) convert current stoichiometric reagents into catalytic systems, and ii) enable more efficient hydride regeneration.[111]

Artificial Photosynthesis. Growing future global energy demands and the influence of increasing atmospheric CO_2 concentrations on earth's climate have inspired researchers over the past few decades to investigate methods by which CO_2 could be photoelectrochemically converted into fuels analogously to natural photosynthesis.[171-174] Mitigation of industrially produced CO_2 may be viable because many processes can recover it in high purity from effluent streams, thus enabling the capture of the greenhouse gas before it is released into the atmosphere.[175] If efficient catalytic approaches to reducing CO_2 from industrial waste streams can be developed, they will offer an attractive alternative to the exorbitant cost of CO_2 sequestration methods for lowering the concentrations of atmospheric CO_2. However, in contrast

to the macroscopic challenges associated with practical CO_2 sequestration, the chemical conversion of CO_2 and solar energy into fuels by artificial photosynthesis poses a number of esoteric, fundamental challenges.

In these artificial photosynthesis approaches, a preferred product of CO_2 reduction is the 6-electron reduced species methanol, an energy-dense liquid fuel that can be safely transported, as opposed to the fully (8-electron) reduced species methane.[176-178] The reduction of CO_2 to CH_3OH is a six-electron, proton-coupled reduction that occurs at a moderate standard reduction potential of -0.39 V versus NHE:[179]

$$CO_2 + 6H^+ + 6e^- \rightarrow CH_3OH + H_2O \qquad (9)$$
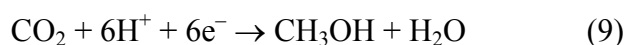
However, stepwise single-electron reduction processes generate reactive open-shell intermediates at every odd reduction. Thus, they are undesirable due to the high energy demands required to produce the radical intermediates of the odd-electron reductions and the corresponding low selectivity of the single-electron reduction process. For example, the first one-electron reduction of CO_2 to the radical anion $CO_2^{\bullet-}$ requires an applied potential of -1.89 V versus NHE.[180] Alternatively, these high-energy odd-electron reduced radical intermediates can be avoided and product selectivity improved if CO_2 reduction were executed using a sequence of three proton-coupled hydride transfer (HT-PT) steps.[111, 153] Each hydride transfer step forms a stable, closed-shell intermediate, such as formic acid or formaldehyde, as illustrated in Scheme 7a.

$$CO_2 + 3H^+ + 3H^- \rightarrow CH_3OH + H_2O \qquad (10)$$
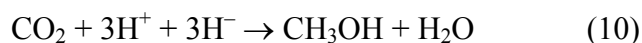
Electrocatalytic and photocatalytic CO_2 reduction by metal-based and metal-free catalysts have been reviewed previously.[21, 179, 181] The following discussion focuses on hydride transfers in artificial photosynthesis, because NADH analogs have been proposed as intermediates in CO_2 (photo)reduction.[153, 182] This section describes recent research efforts in this direction.

Scheme 7. (a) Reduction of CO_2 to methanol by dihydropyridine (PyH_2) catalyst involves three consecutive proton-coupled hydride transfers.[153] Hydridic hydrogens are shown in red and protic hydrogens are shown in blue. (b) Electrochemical regeneration of the active hydride form PyH_2 achieved by sequential protonation and reduction steps.[153]
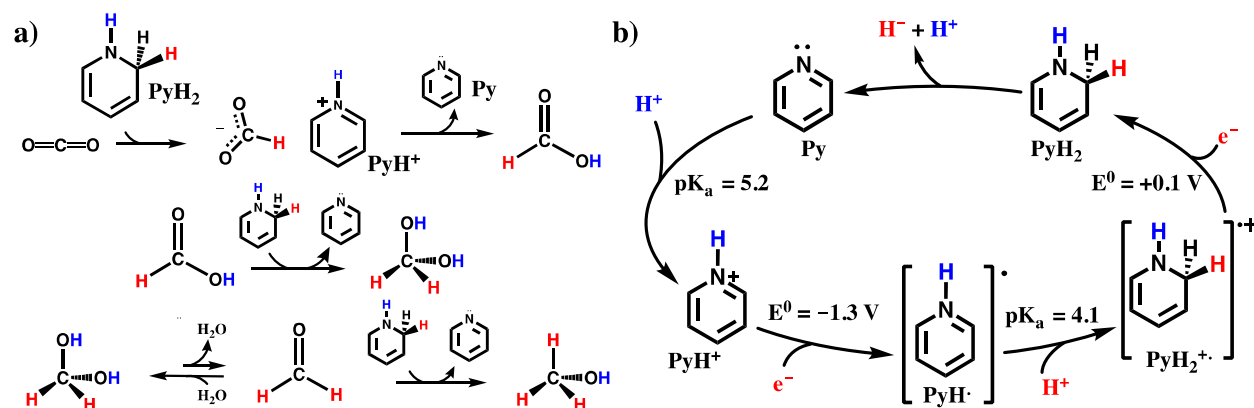
The initial step of catalytic conversion of CO_2 to methanol includes the reduction of CO_2 to formate. Thus, the catalytic hydride must be a stronger hydride donor than formate, which has a ΔG_{H-} of 44 kcal/mol[157] in MeCN and 24[183] (or 35)[184] kcal/mol in water. Furthermore, low activation energies are desired for kinetic viability at room temperature. Hydrosilanes and hydroboranes perform stoichiometric reductions of CO_2 via a hydride transfer mechanism, where Lewis acids are utilized to activate CO_2 for these reduction processes.[185, 186] While the thermodynamic hydricities of hydrosilanes and hydroboranes appear insufficient for hydride transfer to CO_2 ($\Delta G_{H-} > 74$ kcal/mol, Table 2),[92] these hydride transfers occur due to the coupled formation of the respective Si-O or B-O bonds. Thus, the products of CO_2 reduction by silanes, boranes and other FLPs often include methoxy- and formyl-complexes that preclude further catalytic reduction.[187-195] In contrast, Musgrave and coworkers predicted that CO_2 can be catalytically converted to formic acid, and eventually methanol by concerted HT-PT to CO_2 by ammonia-borane (NH_3BH_3).[196, 197] The concerted hydride and proton transfer (HT and PT) steps are driven by the conversion of the B-N dative bond into a B-N covalent bond of $NH_2=BH2$ upon HT and PT. This reaction proceeds with feasible thermodynamics and kinetics due to the stabilization of the B-N bond as it is converted from a dative to covalent bond and the formation of a six-membered ring transition state that includes CO_2.[196, 198] Although ammonia-borane effectively reduces CO_2 and its subsequent reduced intermediates, it is not considered a viable

metal-free catalyst for CO_2 reduction because the oxidized intermediate $NH_2=BH_2$, which is isoelectronic to ethylene, oligomerizes or forms stable 6-member ring structures.[198]

Clear examples of catalytic hydrides are not known, but have been implicated to explain the electrocatalytic and photoelectrocatalytic reduction of CO_2 by organic N-containing heteroaromatic compounds.[111, 199] Specifically, Bocarsly and coworkers have shown that a simple pyridinium ion catalyzes photoelectrochemical CO_2 reduction to methanol at a p-GaP photocathode.[151] They observed that this system achieved near 100% Faradaic efficiency operating at 220 mV of underpotential of an illuminated p-type GaP electrode in water – the most successful reported photoelectrochemical conversion of CO_2 to methanol to date. While their initially proposed mechanism involved the pyridinyl-COOH intermediate,[151, 200, 201] it has been discarded due to several inconsistencies associated with the reduction potentials and pK_a values of relevant intermediates.[111, 182, 199, 201, 202] Subsequent computational studies have shown that a likely mechanism involves the photoelectrochemical formation of dihydropyridine, which then drives CO_2 reduction via a hydride transfer mechanism.[111, 153, 182, 199, 201]

Musgrave and co-workers predicted that dihydropyridine reduces CO_2 via a hydride transfer-proton transfer mechanism where the PTs occur through a water-mediated proton relay mechanism.[111, 153] While the reduction of CO_2 to formic acid involves a sequential HT-PT mechanism, the subsequent steps, reduction of formic acid and formaldehyde, involve coupled HTs and PTs where the PTs occur along the exit channel of the HT reaction, but without a separate transition state with PT character (Scheme 7a). All three of the HT-PT reductions (of CO_2, formic acid and formaldehyde) were predicted to be exergonic with reaction free energies of −5.6, −11.9, and −30.8 kcal/mol in water, respectively, with the largest activation barriers of 18.7 and 20.0 kcal/mol exhibited for the reduction of formic acid and dehydration of the methane diol product of formic acid reduction, respectively.[111] The HTs are driven by the recovery of aromaticity upon hydride donation where the oxidized donor becomes aromatic and significantly more stable, an analogous behavior to that observed in reductions by nature's NADPH hydride, as discussed in the Natural Photosynthesis subsection. The Py/PyH_2 cycle distinguishes its organic aromatic hydride PyH_2 from other metal-free hydrides because it can be recycled

(Scheme 7b). As such, PyH_2 serves as an exemplar for metal-free hydride catalysts, including for the specific reduction of CO_2 into fuels.

After hydride transfer, the active dihydropyridine species can be recovered chemically, photochemically, electrochemically, as represented in Scheme 7b, or photoelectrochemically. Initial protonation of pyridine (Py) to form the pyridinium cation (PyH^+) readily occurs in aqueous medium (pK_a = 5.2).[153] Subsequent one-electron reduction of PyH^+ occurs at a standard potential E^0 of −1.06 V vs NHE,[153] which can be achieved using photogenerated electrons occupying conduction band states of the p-type GaP electrode. The second protonation is more likely to occur at the ortho- position (pK_a = 4.2) than the para- position (pK_a = 2.4).[153] The subsequent reduction to form the desired dihydride species, PyH_2, proceeds with relative ease (E^0 = +0.36 V versus NHE) because it involves neutralization of a radical-cation to form a closed-shell product.[153]

Indirect evidence that NADH analogs play a key role in electrocatalytic CO_2 reduction has been provided using *operando* reflectance FTIR experiments, which showed that the electrochemical reduction of pyridinium ion on a Pt electrode generates piperidine, a fully reduced derivative with formula C_5NH_6.[203] While dihydropyridine was not detected in this study, it is a likely intermediate in the reduction of pyridinium ion to piperidine. Another set of experiments that confirms the role of NADH analogs were performed in a study of the electrocatalytic reduction of CO_2 to methanol on Pt and carbon electrodes, where it was shown that electrocatalysis improves in the presence of dihydrophenanthridine and dihydroacridine derivatives.[204]

Despite the evidence these results provide, direct experimental proof of the homogeneous catalytic reduction of CO_2 by metal-free hydrides has not yet been obtained. For example, attempts to chemically reduce CO_2 using dihydrophenanthridines, dihydroacridines and dihydropyridines did not observe reduction products.[204, 205] Furthermore, electrocatalytic CO_2 reduction by aromatic N-heterocycles exhibits strong dependence on the type of working electrode.[151, 200, 204] These results indicate that the electrode may play a role in the catalysis, either indirectly, for example by influencing competing reactions, such as proton reduction, or directly, for example by interacting with the catalytic species or by catalyzing CO_2 reduction

itself. Keith and Carter proposed that the catalysis of CO_2 reduction by pyridines occurs heterogeneously, where CO_2 is reduced by hydride transfer from surface-bound PyH_2 species.[182] Kronawitter and coworkers propose a competing mechanism where piperidinium-like species, formed through heterogeneous interactions with a Pt electrode, perform the hydride transfer reactions.[203]

Other related organic hydride systems have a similar reactivity to the aforementioned dihydropyridine system. For example, Tanaka and coworkers examined the ruthenium-based catalyst $[Ru(bpy)_2(pbnHH)]^{2+}$ with the organic ligand, pbnHH (2-(pyridin-2-yl)-5,10-dihydrobenzo[b][1,5]naphthyridine), which is similar in structure to dihydropyridines.[206, 207] This hydride was found to catalyze the reduction of CO_2 to formate in the presence of strong carboxylate bases. While $[Ru(bpy)_2(pbnHH)]^{2+}$ is reported to possess a ΔG_{H^-} of ~90 kcal/mol in $MeCN$[86] – making it an extremely weak hydride – its HT is facilitated by: (1) activation by carboxylate bases and (2) further reduction to the triply reduced species $[Ru(bpy)_2^{\bullet-}(pbnHH)]^+$.[86] Another example involves 6,7-dimethyl-4-hydroxy-2-mercaptopteridine (PTE), which was recently reported to catalyze the reduction of CO_2 to methanol on a glassy carbon electrode.[208] Pteridines can cycle analogously to the Py/PyH_2 redox cycle in which HTs are driven by re-aromatization: upon concerted $2H^+/2e^-$ transfer to PTE followed by tautomerization, the dihydropteridine $PTEH_2$ is formed.[209] However, Musgrave and coworkers predicted that although the overall reaction to methanol is exergonic by ~5 kcal/mol, the HTs involved activation barriers as high as 30 kcal/mol,[209] rendering this hydride too slow for feasible kinetics at room temperature, in agreement with Saveant and Tard's experimental observations.[52] The kinetics could possibly improve with proper moiety functionalization, but this has of yet, not been demonstrated. Additionally, Alherz et al. recently reported that benzimidazole-based hydrides are effective for reducing CO_2 via HT.[93] A more detailed study is however required to determine their feasibility as molecular catalysts.

Hydrogenation in Synthetic Chemistry. Metal-free hydride donors are powerful reducing agents utilized in many transformations in organic synthesis.[7, 8, 14, 144-149] The role of metal-free motifs is to either stoichiometrically transfer the hydride ion to activated unsaturated groups or to act as catalysts that activate molecular hydrogen towards reduction of relevant substrates.

Borohydrides and silanes are often used as stoichiometric reagents because the recovery of hydride catalysts is difficult due to: i) very negative reduction potentials of conjugate hydride acceptors,[131, 132] and ii) irreversible bond formation with reduced substrates, for example, to form Si-O and B-O bonds.[7, 14] These stoichiometric reagents are often used in asymmetric hydrogenations, when accompanied with chiral co-catalysts.[20, 210]

Stoichiometric hydride transfer reactions using NADH analogs, such as Hantzsch's esters (entries 92 and 93, $\Delta G_{H-} \sim 60$ kcal/mol and $N = 9$),[40, 78] have been successfully performed on numerous compounds containing activated C=C and C=N functional groups.[20] The kinetics of a hydride transfer to different substrates can be improved using appropriate activation.[6, 20] For example, C=C bonds can be converted into enamines, whereas C=N and C=O bonds can be activated by protonation.[20] While the protonation of C=O bonds is hindered by the very low pK_a value of its protonated form ($pK_a < -3$ in acidic media),[211, 212] successful activation of the carbonyl group can be realized using Lewis acids, such as Eu and Cu ions.[20] Additionally, carbonyl bonds are more difficult to reduce than C=C and C=N bonds, due to the lower hydride affinities of C=O bonds ($\Delta H_{H-} = 20\text{-}50$ kcal/mol)[75] relative to C=C ($\Delta H_{H-} = 50\text{-}60$ kcal/mol)[74] and C=N bonds ($\Delta H_{H-} = 40\text{-}70$ kcal/mol).[213] Although NADH analogs are usually considered stoichiometric agents, several reports demonstrate that these transformations are feasible even with catalytic amounts of the hydride. For example, the recovery of the active hydride form was achieved by chemical reduction with a co-reductant (i.e. dithionite)[214, 215] or by metal-mediated hydride transfers.[216, 217] Specifically, dihydrophenanthridine has been utilized for the reduction of many classes of compounds, such as quinolones, quinoxalines and benzoxazines. These reactions were performed in the catalytic regime, where dihydrophenanthridine was regenerated using H_2 gas in the presence of Ru and Fe-based complexes.[216, 217]

Catalytic hydrogenation has also been successfully achieved using frustrated Lewis pairs (FLPs).[9, 10, 67, 69] As discussed in the Relevance to Catalysis section, FLPs react with molecular hydrogen to form a hydride donor LA-H$^-$ and a proton donor LB-H$^+$. These H_2 adducts then react with substrates containing C=C, C=N and C=O groups in a HT-PT mechanism to form the associated reduced substrates and close the catalytic cycle. While FLPs are successfully utilized

to reduce C=C and C=N bonds, the reduction of C=O groups is hindered by the Lewis acidity of boranes and low pK_a values of carbonyl conjugated acids.[218]

As discussed in the Relevance to Catalysis section, ΔG_{H-} and pK_a values can be utilized to tune the driving force for reversible H_2 activation and successive hydride transfers to substrates (Scheme 5). Table 4 lists selected examples of Lewis pairs utilized for H_2 activation.[70, 144-146, 219-226] In each case, the driving force for H_2 activation was evaluated using the pK_a value of the protonated Lewis base (LB-H$^+$) and thermodynamic hydricity of the Lewis acid-hydride (LA-H$^-$). Lewis pairs with a wide range of pK_a values (–2.5 to 17 in MeCN)[227-230] and ΔG_{H-} values (22-65 kcal/mol in MeCN)[56, 92] are utilized for H_2 activation.

Table 4. Select examples of the applicability of the thermodynamic hydricity of Lewis Acids and pK_a of Lewis Bases for describing the reactivity of different FLPs. See Scheme 5 for details of ΔG_{rxn}.

Lewis Acceptor	ΔG_{H-}[92]	Lewis Base	pK_a	ΔG_{rxn}	Observed Reaction (Substrates)[a]	REF
$B(C_6F_5)_3$	65	NHC-carbene	34[227]	-35	YN	[219, 220]
$B(C_6F_5)_3$	65	iPr_2NH	18[229]	-13.6	YN	[221]
$B(C_6F_5)_3$	65	$P(tBu)_3$	17[229]	-12.2	YN	[222]
$B(C_6F_5)_3$	65	PMe_3	16.6[229]	-11.6	NR	[222]
$B(C_6F_5)_3$	65	2,6-lutidine	14.1[229]	-8.2	YN	[145]
$B(C_6F_5)_3$	65	PPh_3	7.61[229]	0.6	NR	[222]
$B(C_6F_5)_3$	65	$P(napht)_3$	6.9[228]	1.6	YR (C=C)[e]	[144]
$B(C_6F_5)_3$	65	$P(C_6F_5)Ph_2$	3[228]	6.9	YR (C=C)	[144]
$B(C_6F_5)_3$	65	$P(2,6-C_6H_3Cl_2)_3$	2[228]	8.3	YR (C=C)	[144]
$B(C_6F_5)_3$	65	Et_2O	1[b]	9.6	YR (C=O)[e]	[149]
$B(C_6F_5)_3$	65	$P(C_6F_5)_3$	0.7[228]	10.0	NR	[222]
$BCl(C_6F_5)_2$	64.7	$P(tBu)_3$	17	-11.9	YN	[223]
$B(C_6F_4-p-H)_3$	63	$P(tBu)_3$	17	-10.2	YN	[224]
$B(C_6F_4-p-H)_3$	63	PCy_3	16.1[229]	-8.9	YN	[224]
$B(C_6F_4-p-H)_3$	63	$P(p-MeO-Ph)_3$	11[229]	-2.0	YR	[224]
$BPh(C_6F_5)_2$[c]	55	Dimethylaniline[c]	11[229]	6.0	YR (C≡C)[e]	[148]
$B(Ethylbenzene)(C_6F_5)_2$	55	$P(tBu)_3$	17	-2.2	YR	[146]
$B(C_6F_5)_2Ph$[c]	54	NPh_3[c,229]	-2.5	25.4	NR	[225]
$BCy(C_6F_5)_2$	53	$P(tBu)_3$	17	-0.2	YR	[146]
$B(2,6-F-C_6H_3)_3$	51	Collidine	15[d]	4.5	YR (C=C)	[147]
$B(2,6-F-C_6H_3)_3$	51	2,6-lutidine	14.1	5.8	YR (C=C)[e]	[147]
BEt_3	26	2,6-lutidine	14.1	30.8	NR	[145]
$BMes_3$	22.2	$P(tBu)_3$	17	30.6	NR	[145]
$Si(C_6Me5)_3^+$	74	$P(tBu)_3$	17	-21.2	YN	[226]
$Si(C_6Me5)_3^+$	74	PCy_3	16.1	-20.0	YN	[226]
Acr^+	70[56]	2,6-lutidine	14.1	-13.2	YN	[70]

[a] YN – reaction occurs but not reversibly; YR – reaction occurs reversibly; NR – no reaction
[b] Derived from the aqueous pK_a[134, 230]
[c] Intramolecular FLP.
[d] Approximated to have the same values as 2,3-dimethylpyridine.[229]
[e] Requires elevated temperatures.

Table 4 also indicates whether each FLP successfully activated H_2. It is clear from the table that H_2 activation was observed in cases where the estimated ΔG_{rxn} is ~0 to 10 kcal/mol. For example, H_2 cleavage was observed for $B(C_6F_5)_3/P(tBu)_3$, whereas no reaction occurred when a much weaker Lewis base ($P(C_6F_5)_3$) was used.[222] However, ΔG_{rxn} does not fully describe the likelihood of a reaction. Specifically, both $B(C_6F_5)_3/PPh_3$ and $B(C_6F_5)_3/PMe_3$ pairs show favorable thermodynamics for H_2 splitting (ΔG_{rxn}~ 0 kcal/mol), but the formation of a Lewis acid-base adduct prevents further reaction.[222] Furthermore, reversible reactions have been observed for FLPs with ΔG_{rxn} that varies from –10 to 5 kcal/mol, as exemplified by $B(C_6F_5)_3$-$/P(napht)_3$ and $B(2,6-F-C_6H_3)_3/lut$ pairs, which have been utilized in catalytic C=C bond reduction.[144, 147] Predictions for efficient H_2 cleavage using pK_a and ΔG_{H-} parameters can be

expanded to other Lewis acids, such as $Si(C_6Me_5)_3^+$ and methyl-acridinium, as shown in Table 4.[70, 226] This analysis shows how thermodynamic hydricity values collected in this review can be utilized to tune the reactivity of FLP catalysts.

VII. Conclusions and Future Outlook

In summary, the thermodynamic and kinetic hydricity parameters can in principle guide the design of hydride donors with desirable properties for specific chemical reductions. Analyzing trends between ΔG_{H^-} and other important properties, such as the nucleophilicity (N) and the first and second reduction potentials (E_1 and E_2), uncovers the principles that govern chemical reductions by hydride transfers to understand and enable the design of hydrides to perform desired reductions. For instance, structural and electronic features, such as rearomatization and hydride bond polarity, were found to considerably affect hydride transfer. Exploiting these effects systematically allows for the design of hydride donors that balance the energy efficiency and kinetics of hydride transfer reductions, including the ability to design for catalytic over stoichiometric mechanisms for chemical reductions.

A major challenge to utilizing metal-free hydrides for catalytic chemical reductions is the difficulty of recovering the active catalyst. Specifically, B- and Si-based hydrides undergo the irreversible formation of B-O and Si-O bonds in the process of reducing C=O bonds, which are very stable and thus difficult to dissociate to recover the reducing agent. To overcome this challenge, utilizing hydrides of similar thermodynamic hydricity but weaker Lewis acidity is recommended. Electrocatalysts, on the other hand, require large negative reduction potentials to regenerate the hydride. Additionally, a significant tradeoff is observed between the strength of the hydride donor and the first reduction potential as a consequence of the scaling relation between ΔG_{H^-} and E_1. Breaking this scaling relation is key to synthesizing catalysts that can utilize less energy, require smaller over-potentials and yet be kinetically competent by maintaining the same reduction prowess. However, decoupling the strength of the hydride donor from the potential required for its recovery is a daunting challenge. In natural systems, high-energy intermediates are avoided by coupling proton and electron transfers as with the reduction

of FAD to $FADH_2$. Another approach involves the incorporation of metal ions, where the role of the metal is to tune the reduction potential of the coordinated hydride donor.

Corresponding Author

*glusac@uic.edu

ORCID

Ksenija D. Glusac: 0000-0002-2734-057X

Charles B. Musgrave: 0000-0002-5732-3180

Stefan Ilic: 0000-0002-6305-4001

Abdulaziz Alherz: 0000-0001-7529-3483

References

1. E. S. Wiedner, M. B. Chambers, C. L. Pitman, R. M. Bullock, A. J. Miller and A. M. Appel, *Chemical Reviews*, 2016, **116**, 8655-8692.
2. D. L. DuBois, *Inorganic Chemistry*, 2014, **53**, 3935-3960.
3. Y. Kan and Q. Zhang, in *Nanostructured Materials for Next-Generation Energy Storage and Conversion*, Springer, 2017, ch. Transition Metal Complexes for Hydrogen Activation, pp. 43-84.
4. R. B. Gordon, M. Bertram and T. E. Graedel, *Proceedings of the National Academy of Sciences*, 2006, **103**, 1209-1214.
5. J. M. Berg, J. L. Tymoczko and L. Stryer, in *Biochemistry*, New York: WH Freeman, 2002.
6. A. McSkimming and S. B. Colbran, *Chemical Society Reviews*, 2013, **42**, 5439-5488.
7. H. C. Brown and S. Krishnamurthy, *Tetrahedron*, 1979, **35**, 567-607.

8.   H. C. Brown, S. Kim and S. Krishnamurthy, *The Journal of Organic Chemistry*, 1980, **45**, 1-12.
9.   D. W. Stephan and G. Erker, *Angewandte Chemie International Edition*, 2010, **49**, 46-76.
10.   D. W. Stephan and G. Erker, *Angewandte Chemie International Edition*, 2015, **54**, 6400-6441.
11.   C. M. Visser, *Origins of Life and Evolution of Biospheres*, 1982, **12**, 165-179.
12.   C. Walsh, *Accounts of Chemical Research*, 1986, **19**, 216-221.
13.   R. Li, M. A. Bianchet, P. Talalay and L. M. Amzel, *Proceedings of the National Academy of Sciences*, 1995, **92**, 8846-8850.
14.   G. L Larson and J. L Fry, *Ionic and Organometallic-Catalyzed Organosilane Reductions*, Wiley Online Library, 2008.
15.   S. Burck, D. Gudat, M. Nieger and W.-W. Du Mont, *Journal of the American Chemical Society*, 2006, **128**, 3946-3955.
16.   D. Quane and R. S. Bottei, *Chemical Reviews*, 1963, **63**, 403-442.
17.   A. Osuka, H. Shimizu and H. Suzuki, *Chemistry Letters*, 1983, **12**, 1373-1374.
18.   H. Mayr and M. Patz, *Angewandte Chemie International Edition*, 1994, **33**, 938-957.
19.   M. Horn, L. H. Schappele, G. Lang-Wittkowski, H. Mayr and A. R. Ofial, *Chemistry-A European Journal*, 2013, **19**, 249-263.
20.   C. Zheng and S.-L. You, *Chemical Society Reviews*, 2012, **41**, 2498-2518.
21.   Y. Oh and X. Hu, *Chemical Society Reviews*, 2013, **42**, 2253-2261.
22.   K. L. Handoo, J. P. Cheng and V. D. Parker, *Journal of the American Chemical Society*, 1993, **115**, 5067-5072.
23.   Y. Matsubara, S. E. Hightower, J. Chen, D. C. Grills, D. E. Polyansky, J. T. Muckerman, K. Tanaka and E. Fujita, *Chemical Communications*, 2014, **50**, 728-730.
24.   Y. Matsubara, E. Fujita, M. D. Doherty, J. T. Muckerman and C. Creutz, *Journal of the American Chemical Society*, 2012, **134**, 15743-15757.
25.   S. M. Barrett, C. L. Pitman, A. G. Walden and A. J. Miller, *Journal of the American Chemical Society*, 2014, **136**, 14718-14721.
26.   D. E. Berning, B. C. Noll and D. L. DuBois, *Journal of the American Chemical Society*, 1999, **121**, 11432-11447.
27.   J. Y. Yang, S. E. Smith, T. Liu, W. G. Dougherty, W. A. Hoffert, W. S. Kassel, M. R. DuBois, D. L. DuBois and R. M. Bullock, *Journal of the American Chemical Society*, 2013, **135**, 9700-9712.
28.   C. J. Curtis, A. Miedaner, W. W. Ellis and D. L. DuBois, *Journal of the American Chemical Society*, 2002, **124**, 1918-1925.
29.   R. Ciancanelli, B. C. Noll, D. L. DuBois and M. R. DuBois, *Journal of the American Chemical Society*, 2002, **124**, 2984-2992.
30.   D. P. Estes, A. K. Vannucci, A. R. Hall, D. L. Lichtenberger and J. R. Norton, *Organometallics*, 2011, **30**, 3444-3447.
31.   D. E. Berning, A. Miedaner, C. J. Curtis, B. C. Noll, M. C. Rakowski DuBois and D. L. DuBois, *Organometallics*, 2001, **20**, 1832-1839.
32.   J. W. Raebiger, A. Miedaner, C. J. Curtis, S. M. Miller, O. P. Anderson and D. L. DuBois, *Journal of the American Chemical Society*, 2004, **126**, 5502-5514.
33.   J. Y. Yang, R. M. Bullock, W. J. Shaw, B. Twamley, K. Fraze, M. R. DuBois and D. L. DuBois, *Journal of the American Chemical Society*, 2009, **131**, 5935-5945.

34. A. Miedaner, J. W. Raebiger, C. J. Curtis, S. M. Miller and D. L. DuBois, *Organometallics*, 2004, **23**, 2670-2679.

35. J. A. Roberts, A. M. Appel, D. L. DuBois and R. M. Bullock, *Journal of the American Chemical Society*, 2011, **133**, 14604-14613.

36. V. Parker, *Acta Chemica Scandinavica*, 1992, **46**, 1133-1134.

37. J. Cheng, K. L. Handoo and V. D. Parker, *Journal of the American Chemical Society*, 1993, **115**, 2655-2660.

38. J. Cheng, K. L. Handoo, J. Xue and V. D. Parker, *The Journal of Organic Chemistry*, 1993, **58**, 5050-5054.

39. X.-M. Zhang, J. W. Bruno and E. Enyinnaya, *The Journal of Organic Chemistry*, 1998, **63**, 4671-4678.

40. S. Ilic, U. Pandey Kadel, Y. Basdogan, J. A. Keith and K. D. Glusac, *Journal of the American Chemical Society*, Submitted.

41. D. D. Wayner and V. D. Parker, *Accounts of Chemical Research*, 1993, **26**, 287-294.

42. J. Walpita, X. Yang, R. Khatmullin, H. L. Luk, C. M. Hadad and K. D. Glusac, *Journal of Physical Organic Chemistry*, 2016, **29**, 204-208.

43. V. D. Parker, K. L. Handoo, F. Roness and M. Tilset, *Journal of the American Chemical Society*, 1991, **113**, 7493-7498.

44. H. G. Roth, N. A. Romero and D. A. Nicewicz, *Synlett*, 2016, **27**, 714-723.

45. X.-Q. Zhu, J.-Y. Zhang and J.-P. Cheng, *The Journal of Organic Chemistry*, 2006, **71**, 7007-7015.

46. X.-Q. Zhu, Y. Tan and C.-T. Cao, *The Journal of Physical Chemistry B*, 2010, **114**, 2058-2075.

47. X.-Q. Zhu, M.-T. Zhang, A. Yu, C.-H. Wang and J.-P. Cheng, *Journal of the American Chemical Society*, 2008, **130**, 2501-2516.

48. X. Han, W. Hao, X.-Q. Zhu and V. D. Parker, *The Journal of Organic Chemistry*, 2012, **77**, 6520-6529.

49. J.-P. Cheng, Y. Lu, X. Zhu and L. Mu, *The Journal of Organic Chemistry*, 1998, **63**, 6108-6114.

50. P. K. Giesbrecht, D. B. Nemez and D. E. Herbert, *Chemical Communications*, 2018, **54**, 338-341.

51. A. Anne and J. Moiroux, *The Journal of Organic Chemistry*, 1990, **55**, 4608-4614.

52. J.-M. Saveant and C. d. Tard, *Journal of the American Chemical Society*, 2016, **138**, 1017-1021.

53. F. G. Bordwell, *Accounts of Chemical Research*, 1988, **21**, 456-463.

54. O. Hammerich and B. Speiser, *Organic Electrochemistry: Revised and Expanded*, CRC Press, 2015.

55. R. H. Morris, *Chemical Reviews*, 2016, **116**, 8588-8654.

56. W. W. Ellis, J. W. Raebiger, C. J. Curtis, J. W. Bruno and D. L. DuBois, *Journal of the American Chemical Society*, 2004, **126**, 2738-2743.

57. D. L. DuBois, D. M. Blake, A. Miedaner, C. J. Curtis, M. R. DuBois, J. A. Franz and J. C. Linehan, *Organometallics*, 2006, **25**, 4414-4419.

58. R. Roberts, D. Ostović and M. Kreevoy, *Faraday Discussions of the Chemical Society*, 1982, **74**, 257-265.

59. M. M. Kreevoy and I. S. H. Lee, *Journal of the American Chemical Society*, 1984, **106**, 2550-2553.

60.   M. M. Kreevoy, D. Ostovic, I. S. H. Lee, D. A. Binder and G. W. King, *Journal of the American Chemical Society*, 1988, **110**, 524-530.

61.   B. R. Galan, J. Schöffel, J. C. Linehan, C. Seu, A. M. Appel, J. A. Roberts, M. L. Helm, U. J. Kilgore, J. Y. Yang and D. L. DuBois, *Journal of the American Chemical Society*, 2011, **133**, 12767-12779.

62.   C. Tsay, B. N. Livesay, S. Ruelas and J. Y. Yang, *Journal of the American Chemical Society*, 2015, **137**, 14114-14121.

63.   J. W. Raebiger and D. L. DuBois, *Organometallics*, 2005, **24**, 110-118.

64.   Y. Hu and J. R. Norton, *Journal of the American Chemical Society*, 2014, **136**, 5938-5948.

65.   A. J. Price, R. Ciancanelli, B. C. Noll, C. J. Curtis, D. L. DuBois and M. R. DuBois, *Organometallics*, 2002, **21**, 4833-4839.

66.   A. M. Lilio, M. H. Reineke, C. E. Moore, A. L. Rheingold, M. K. Takase and C. P. Kubiak, *Journal of the American Chemical Society*, 2015, **137**, 8251-8260.

67.   D. W. Stephan, *Journal of the American Chemical Society*, 2015, **137**, 10018-10032.

68.   G. Erker and D. W. Stephan, *Frustrated Lewis Pairs*, Springer, 2013.

69.   D. W. Stephan, *Organic & Biomolecular Chemistry*, 2008, **6**, 1535-1539.

70.   E. R. Clark and M. J. Ingleson, *Angewandte Chemie International Edition*, 2014, **53**, 11306-11309.

71.   E. J. Lawrence, E. R. Clark, L. D. Curless, J. M. Courtney, R. J. Blagg, M. J. Ingleson and G. G. Wildgoose, *Chemical Science*, 2016, **7**, 2537-2543.

72.   X. Q. Zhu, H. R. Li, Q. Li, T. Ai, J. Y. Lu, Y. Yang and J. P. Cheng, *Chemistry-A European Journal*, 2003, **9**, 871-880.

73.   X.-Q. Zhu, Z. Dai, A. Yu, S. Wu and J.-P. Cheng, *The Journal of Physical Chemistry B*, 2008, **112**, 11694-11707.

74.   X. Q. Zhu, M. Zhang, Q. Y. Liu, X. X. Wang, J. Y. Zhang and J. P. Cheng, *Angewandte Chemie International Edition*, 2006, **45**, 3954-3957.

75.   X.-Q. Zhu, X. Chen and L.-R. Mei, *Organic Letters*, 2011, **13**, 2456-2459.

76.   X. Q. Zhu, L. Cao, Y. Liu, Y. Yang, J. Y. Lu, J. S. Wang and J. P. Cheng, *Chemistry-A European Journal*, 2003, **9**, 3937-3945.

77.   A. Karkamkar, K. Parab, D. M. Camaioni, D. Neiner, H. Cho, T. K. Nielsen and T. Autrey, *Dalton Transactions*, 2013, **42**, 615-619.

78.   D. Richter and H. Mayr, *Angewandte Chemie International Edition*, 2009, **48**, 1958-1961.

79.   M. A. Funke and H. Mayr, *Chemistry-A European Journal*, 1997, **3**, 1214-1222.

80.   H. Mayr, G. Lang and A. R. Ofial, *Journal of the American Chemical Society*, 2002, **124**, 4076-4083.

81.   D. Richter, Y. Tan, A. Antipova, X. Q. Zhu and H. Mayr, *Chemistry–An Asian Journal*, 2009, **4**, 1824-1829.

82.   M. Horn, H. Mayr, E. Lacôte, E. Merling, J. Deaner, S. Wells, T. McFadden and D. P. Curran, *Organic Letters*, 2011, **14**, 82-85.

83.   H. Mayr, T. Bug, M. F. Gotta, N. Hering, B. Irrgang, B. Janker, B. Kempf, R. Loos, A. R. Ofial and G. Remennikov, *Journal of the American Chemical Society*, 2001, **123**, 9500-9512.

84.   E.-U. Würthwein, G. Lang, L. H. Schappele and H. Mayr, *Journal of the American Chemical Society*, 2002, **124**, 4084-4092.

85. X. Yang, J. Walpita, D. Zhou, H. L. Luk, S. Vyas, R. S. Khnayzer, S. C. Tiwari, K. Diri, C. M. Hadad and F. N. Castellano, *The Journal of Physical Chemistry B*, 2013, **117**, 15290-15296.

86. J. T. Muckerman, P. Achord, C. Creutz, D. E. Polyansky and E. Fujita, *Proceedings of the National Academy of Sciences*, 2012, **109**, 15657-15662.

87. X.-J. Qi, Y. Fu, L. Liu and Q.-X. Guo, *Organometallics*, 2007, **26**, 4197-4203.

88. J. Shi, X.-Y. Huang, H.-J. Wang and Y. Fu, *Journal of Chemical Information and Modeling*, 2011, **52**, 63-75.

89. X.-Q. Zhu and C.-H. Wang, *The Journal of Physical Chemistry A*, 2010, **114**, 13244-13256.

90. X.-Q. Zhu, C.-H. Wang, H. Liang and J.-P. Cheng, *The Journal of Organic Chemistry*, 2007, **72**, 945-956.

91. M. T. Mock, R. G. Potter, D. M. Camaioni, J. Li, W. G. Dougherty, W. S. Kassel, B. Twamley and D. L. DuBois, *Journal of the American Chemical Society*, 2009, **131**, 14454-14465.

92. Z. M. Heiden and A. P. Lathem, *Organometallics*, 2015, **34**, 1818-1827.

93. A. Alherz, C.-H. Lim, J. T. Hynes and C. B. Musgrave, *The Journal of Physical Chemistry B*, 2018, **122**, 1278-1288.

94. Y. Zhao and D. G. Truhlar, *Accounts of Chemical Research*, 2008, **41**, 157-167.

95. L. Goerigk and S. Grimme, *Physical Chemistry Chemical Physics*, 2011, **13**, 6670-6688.

96. L. Goerigk and S. Grimme, *Journal of Chemical Theory and Computation*, 2010, **7**, 291-309.

97. J. Tomasi, B. Mennucci and R. Cammi, *Chemical Reviews*, 2005, **105**, 2999-3094.

98. M. Cossi, N. Rega, G. Scalmani and V. Barone, *Journal of Computational Chemistry*, 2003, **24**, 669-681.

99. S. Miertuš, E. Scrocco and J. Tomasi, *Chemical Physics*, 1981, **55**, 117-129.

100. J. Tomasi and M. Persico, *Chemical Reviews*, 1994, **94**, 2027-2094.

101. C. J. Cramer and D. G. Truhlar, *Chemical Reviews*, 1999, **99**, 2161-2200.

102. G. Kovács and I. Pápai, *Organometallics*, 2006, **25**, 820-825.

103. E. Nikitina, V. Sulimov, F. Grigoriev, O. Kondakova and S. Luschekina, *International Journal of Quantum Chemistry*, 2006, **106**, 1943-1963.

104. B. Thapa and H. B. Schlegel, *The Journal of Physical Chemistry A*, 2016, **120**, 5726-5735.

105. L.-P. Wang and T. Van Voorhis, *Journal of Chemical Theory and Computation*, 2012, **8**, 610-617.

106. W. Kohn and L. J. Sham, *Physical Review*, 1965, **140**, A1133.

107. S.-B. Kang, Y.-S. Cho and S.-G. Hwang, *Bulletin of the Korean Chemical Society*, 2009, **30**, 2927-2929.

108. B. Mondal, F. Neese and S. Ye, *Inorganic Chemistry*, 2016, **55**, 5438-5444.

109. M. R. Nimlos, C. H. Chang, C. J. Curtis, A. Miedaner, H. M. Pilath and D. L. DuBois, *Organometallics*, 2008, **27**, 2715-2722.

110. Y.-S. Cho, J.-B. Lee and S.-G. Hwang, *Bulletin of the Korean Chemical Society*, 2012, **33**, 1413-1415.

111. C.-H. Lim, A. M. Holder, J. T. Hynes and C. B. Musgrave, *Journal of the American Chemical Society*, 2014, **136**, 16081-16095.

112. R. Skyner, J. McDonagh, C. Groom, T. van Mourik and J. Mitchell, *Physical Chemistry Chemical Physics*, 2015, **17**, 6174-6191.

113. K. R. Brereton, S. M. Bellows, H. Fallah, A. A. Lopez, R. M. Adams, A. J. Miller, W. D. Jones and T. R. Cundari, *The Journal of Physical Chemistry B*, 2016, **120**, 12911-12919.

114. C. L. Pitman, K. R. Brereton and A. J. Miller, *Journal of the American Chemical Society*, 2016, **138**, 2252-2260.

115. T. W. Bentley, *Angewandte Chemie*, 2011, **123**, 3688-3691.

116. T. W. Bentley, *Journal of Physical Organic Chemistry*, 2011, **24**, 282-291.

117. R. P. Bell, *Proceedings of the Royal Society of London. Series A, Mathematical and Physical Sciences*, 1936, **154**, 414-429.

118. M. Evans and M. Polanyi, *Transactions of the Faraday Society*, 1936, **32**, 1333-1360.

119. S. Pratihar, *Organic & Biomolecular Chemistry*, 2014, **12**, 5781-5788.

120. S.-i. Kiyooka, D. Kaneno and R. Fujiyama, *Tetrahedron*, 2013, **69**, 4247-4258.

121. C. Lee, W. Yang and R. G. Parr, *Physical Review B*, 1988, **37**, 785.

122. B. Miehlich, A. Savin, H. Stoll and H. Preuss, *Chemical Physics Letters*, 1989, **157**, 200-206.

123. T. H. Dunning Jr and P. J. Hay, in *Methods of Electronic Structure Theory*, Springer, 1977, pp. 1-27.

124. A. McLean and G. Chandler, *The Journal of Chemical Physics*, 1980, **72**, 5639-5648.

125. M. J. Frisch, J. A. Pople and J. S. Binkley, *The Journal of Chemical Physics*, 1984, **80**, 3265-3269.

126. D. C. Montgomery and G. C. Runger, *Applied statistics and probability for engineers*, John Wiley & Sons, 2010.

127. H. Mayr, N. Basso and G. Hagen, *Journal of the American Chemical Society*, 1992, **114**, 3060-3066.

128. T. Hiromoto, E. Warkentin, J. Moll, U. Ermler and S. Shima, *Angewandte Chemie International Edition*, 2009, **48**, 6457-6460.

129. C. Douvris and O. V. Ozerov, *Science*, 2008, **321**, 1188-1190.

130. A. Schäfer, M. Reißmann, A. Schäfer, W. Saak, D. Haase and T. Müller, *Angewandte Chemie International Edition*, 2011, **50**, 12636-12638.

131. S. A. Cummings, M. Iimura, C. J. Harlan, R. J. Kwaan, I. V. Trieu, J. R. Norton, B. M. Bridgewater, F. Jäkle, A. Sundararaman and M. Tilset, *Organometallics*, 2006, **25**, 1565-1568.

132. T. J. DuPont and J. L. Mills, *Journal of the American Chemical Society*, 1975, **97**, 6375-6382.

133. D. J. Pasto, V. Balasubramaniyan and P. Wojtkowski, *Inorganic Chemistry*, 1969, **8**, 594-598.

134. B. G. Cox, in *Acids and Bases: Solvent Effects on Acid-Base Strength*, OUP Oxford, 2013.

135. G. Wilkinson, F. G. A. Stone and E. W. Abel, *Comprehensive organometallic chemistry*, Pergamon Press, 1982.

136. I.-S. H. Lee, E. H. Jeoung and M. M. Kreevoy, *Journal of the American Chemical Society*, 1997, **119**, 2722-2728.

137. R. A. Marcus, *The Journal of Physical Chemistry*, 1968, **72**, 891-899.

138. R. Marcus, *The Journal of Physical Chemistry A*, 1997, **101**, 4072-4087.

139. Y. S. Kong and A. Warshel, *Journal of the American Chemical Society*, 1995, **117**, 6234-6242.

140. E. Rosta and A. Warshel, *Journal of Chemical Theory and Computation*, 2012, **8**, 3574-3585.

141. C. F. Bernasconi, *Accounts of Chemical Research*, 1987, **20**, 301-308.

142. B. M. Ceballos, C. Tsay and J. Y. Yang, *Chemical Communications*, 2017.

143. K.-W. Huang, J. H. Han, C. B. Musgrave and E. Fujita, *Organometallics*, 2007, **26**, 508-513.

144. L. Greb, P. Oña-Burgos, B. Schirmer, S. Grimme, D. W. Stephan and J. Paradies, *Angewandte Chemie*, 2012, **124**, 10311-10315.

145. S. J. Geier and D. W. Stephan, *Journal of the American Chemical Society*, 2009, **131**, 3476-3477.

146. C. Jiang, O. Blacque, T. Fox and H. Berke, *Dalton Transactions*, 2011, **40**, 1091-1097.

147. L. Greb, C. G. Daniliuc, K. Bergander and J. Paradies, *Angewandte Chemie International Edition*, 2013, **52**, 5876-5879.

148. K. Chernichenko, Á. Madarász, I. Pápai, M. Nieger, M. Leskelä and T. Repo, *Nature Chemistry*, 2013, **5**, 718-723.

149. T. Mahdi and D. W. Stephan, *Journal of the American Chemical Society*, 2014, **136**, 15809-15812.

150. G. Seshadri, C. Lin and A. B. Bocarsly, *Journal of Electroanalytical Chemistry*, 1994, **372**, 145-150.

151. E. E. Barton, D. M. Rampulla and A. B. Bocarsly, *Journal of the American Chemical Society*, 2008, **130**, 6342-6344.

152. A. Dolganov, B. Tanaseichuk, D. Moiseeva, V. Yurova, J. Sakanyan, N. Shmelkova and V. Lobanov, *Electrochemistry Communications*, 2016, **68**, 59-61.

153. C.-H. Lim, A. M. Holder, J. T. Hynes and C. B. Musgrave, *The Journal of Physical Chemistry Letters*, 2015, **6**, 5078-5092.

154. G. D. Frey, V. Lavallo, B. Donnadieu, W. W. Schoeller and G. Bertrand, *Science*, 2007, **316**, 439-441.

155. G. C. Welch, R. R. San Juan, J. D. Masuda and D. W. Stephan, *Science*, 2006, **314**, 1124-1126.

156. T. A. Rokob, A. Hamza and I. Pápai, *Journal of the American Chemical Society*, 2009, **131**, 10701-10710.

157. D. L. DuBois and D. E. Berning, *Applied Organometallic Chemistry*, 2000, **14**, 860-862.

158. M. Fang, E. S. Wiedner, W. G. Dougherty, W. S. Kassel, T. Liu, D. L. DuBois and R. M. Bullock, *Organometallics*, 2014, **33**, 5820-5833.

159. W. J. Bowyer and W. E. Geiger, *Journal of the American Chemical Society*, 1985, **107**, 5657-5663.

160. K. Fraze, A. D. Wilson, A. M. Appel, M. Rakowski DuBois and D. L. DuBois, *Organometallics*, 2007, **26**, 3918-3924.

161. M. L. Helm, M. P. Stewart, R. M. Bullock, M. R. DuBois and D. L. DuBois, *Science*, 2011, **333**, 863-866.

162. N. Carrillo and E. A. Ceccarelli, *European Journal of Biochemistry*, 2003, **270**, 1900-1915.

163. A. Call, Z. Codolà, F. Acuña-Parés and J. Lloret-Fillol, *Chemistry-A European Journal*, 2014, **20**, 6171-6183.

164.   E. J. Thompson and L. A. Berben, *Angewandte Chemie International Edition*, 2015, **54**, 11642-11646.

165.   G. Schneider, Y. Lindqvist and C.-I. Branden, *Annual Review of Biophysics and Biomolecular Structure*, 1992, **21**, 119-143.

166.   F. Talfournier, N. Colloc'h, J. P. Mornon and G. Branlant, *The FEBS Journal*, 1998, **252**, 447-457.

167.   P. Karplus, M. Daniels and J. HERRIOGI, *Enzyme*, 1991, **10**, 20.

168.   N. Cassan, B. Lagoutte and P. Sétif, *Journal of Biological Chemistry*, 2005, **280**, 25960-25972.

169.   W. Buckel and R. K. Thauer, *Biochimica et Biophysica Acta (BBA)-Bioenergetics*, 2013, **1827**, 94-113.

170.   R. F. Anderson, *Biochimica et Biophysica Acta (BBA)-Bioenergetics*, 1980, **590**, 277-281.

171.   H. Arakawa, M. Aresta, J. N. Armor, M. A. Barteau, E. J. Beckman, A. T. Bell, J. E. Bercaw, C. Creutz, E. Dinjus and D. A. Dixon, *Chemical Reviews*, 2001, **101**, 953-996.

172.   B. Kumar, M. Llorente, J. Froehlich, T. Dang, A. Sathrum and C. P. Kubiak, *Annual Review of Physical Chemistry*, 2012, **63**, 541-569.

173.   A. J. Morris, G. J. Meyer and E. Fujita, *Accounts of Chemical Research*, 2009, **42**, 1983-1994.

174.   N. S. Lewis and D. G. Nocera, *Proceedings of the National Academy of Sciences*, 2006, **103**, 15729-15735.

175.   C. Ampelli, G. Centi, R. Passalacqua and S. Perathoner, *Energy & Environmental Science*, 2010, **3**, 292-301.

176.   G. A. Olah, A. Goeppert and G. S. Prakash, *The Journal of Organic Chemistry*, 2008, **74**, 487-498.

177.   G. A. Olah, G. S. Prakash and A. Goeppert, *Journal of the American Chemical Society*, 2011, **133**, 12881-12898.

178.   Z. Jiang, T. Xiao, V. á. Kuznetsov and P. á. Edwards, *Philosophical Transactions of the Royal Society of London A: Mathematical, Physical and Engineering Sciences*, 2010, **368**, 3343-3364.

179.   J. L. White, M. F. Baruch, J. E. Pander III, Y. Hu, I. C. Fortmeyer, J. E. Park, T. Zhang, K. Liao, J. Gu and Y. Yan, *Chemical Reviews*, 2015, **115**, 12888-12935.

180.   H. Schwarz and R. Dodson, *The Journal of Physical Chemistry*, 1989, **93**, 409-414.

181.   J. Qiao, Y. Liu, F. Hong and J. Zhang, *Chemical Society Reviews*, 2014, **43**, 631-675.

182.   J. A. Keith and E. A. Carter, *The Journal of Physical Chemistry Letters*, 2013, **4**, 4058-4063.

183.   S. J. Connelly, E. S. Wiedner and A. M. Appel, *Dalton Transactions*, 2015, **44**, 5933-5938.

184.   C. Creutz and M. H. Chou, *Journal of the American Chemical Society*, 2009, **131**, 2794-2795.

185.   S. N. Riduan, Y. Zhang and J. Y. Ying, *Angewandte Chemie*, 2009, **121**, 3372-3375.

186.   M.-A. Courtemanche, M.-A. Légaré, L. Maron and F.-G. Fontaine, *Journal of the American Chemical Society*, 2014, **136**, 10708-10717.

187.   T. Matsuo and H. Kawaguchi, *Journal of the American Chemical Society*, 2006, **128**, 12362-12363.

188. A. Berkefeld, W. E. Piers and M. Parvez, *Journal of the American Chemical Society*, 2010, **132**, 10660-10661.

189. G. Ménard and D. W. Stephan, *Angewandte Chemie*, 2011, **123**, 8546-8549.

190. G. Ménard and D. W. Stephan, *Journal of the American Chemical Society*, 2010, **132**, 1796-1797.

191. A. E. Ashley, A. L. Thompson and D. O'Hare, *Angewandte Chemie International Edition*, 2009, **48**, 9839-9843.

192. M.-A. Courtemanche, M.-A. Légaré, L. Maron and F. d. r.-G. Fontaine, *Journal of the American Chemical Society*, 2013, **135**, 9326-9329.

193. T. Wang and D. W. Stephan, *Chemistry-A European Journal*, 2014, **20**, 3036-3039.

194. M. J. Sgro, J. Dömer and D. W. Stephan, *Chemical Communications*, 2012, **48**, 7253-7255.

195. M.-A. Courtemanche, A. P. Pulis, É. Rochette, M.-A. Légaré, D. W. Stephan and F.-G. Fontaine, *Chemical Communications*, 2015, **51**, 9797-9800.

196. P. M. Zimmerman, Z. Zhang and C. B. Musgrave, *Inorganic Chemistry*, 2010, **49**, 8724-8728.

197. L. Roy, P. M. Zimmerman and A. Paul, *Chemistry-A European Journal*, 2011, **17**, 435-439.

198. M. W. Li, I. M. Pendleton, A. J. Nett and P. M. Zimmerman, *The Journal of Physical Chemistry A*, 2016, **120**, 1135-1144.

199. J. A. Keith and E. A. Carter, *Chemical Science*, 2013, **4**, 1490-1496.

200. A. J. Morris, R. T. McGibbon and A. B. Bocarsly, *ChemSusChem*, 2011, **4**, 191-196.

201. C.-H. Lim, A. M. Holder and C. B. Musgrave, *Journal of the American Chemical Society*, 2012, **135**, 142-154.

202. J. A. Keith and E. A. Carter, *Journal of the American Chemical Society*, 2012, **134**, 7580-7583.

203. C. Kronawitter, Z. Chen, P. Zhao, X. Yang and B. Koel, *Catalysis Science & Technology*, 2017, **7**, 831-837.

204. P. K. Giesbrecht and D. E. Herbert, *ACS Energy Letters*, 2017, **2**, 549-555.

205. Y. Yan, E. L. Zeitler, J. Gu, Y. Hu and A. B. Bocarsly, *Journal of the American Chemical Society*, 2013, **135**, 14020-14023.

206. H. Ohtsu and K. Tanaka, *Angewandte Chemie International Edition*, 2012, **51**, 9792-9795.

207. H. Ohtsu, K. Tsuge and K. Tanaka, *Journal of Photochemistry and Photobiology A: Chemistry*, 2015, **313**, 163-167.

208. D. Xiang, D. Magana and R. B. Dyer, *Journal of the American Chemical Society*, 2014, **136**, 14007-14010.

209. C.-H. Lim, A. M. Holder, J. T. Hynes and C. B. Musgrave, *Journal of Physical Chemistry B*, 2017, **121**, 4158-4167.

210. E. M. Carreira, V. K. Aggarwal, N. Arai, E. Bergin and A. B. Santanilla, *Science of Synthesis: Stereoselective Synthesis Vol. 2: Stereoselective Reactions of Carbonyl and Imino Groups*, Georg Thieme Verlag, 2014.

211. K. Yates and R. Stewart, *Canadian Journal of Chemistry*, 1959, **37**, 664-671.

212. E. M. Arnett, R. P. Quirk and J. W. Larsen, *Journal of the American Chemical Society*, 1970, **92**, 3977-3984.

213.   X.-Q. Zhu, Q.-Y. Liu, Q. Chen and L.-R. Mei, *The Journal of Organic Chemistry*, 2009, **75**, 789-808.
214.   B. Procuranti and S. J. Connon, *Chemical Communications*, 2007, 1421-1423.
215.   H.-J. Xu, Y.-C. Liu, Y. Fu and Y.-D. Wu, *Organic Letters*, 2006, **8**, 3449-3451.
216.   Q.-A. Chen, M.-W. Chen, C.-B. Yu, L. Shi, D.-S. Wang, Y. Yang and Y.-G. Zhou, *Journal of the American Chemical Society*, 2011, **133**, 16432-16435.
217.   H. C. Lo and R. H. Fish, *Angewandte Chemie International Edition*, 2002, **41**, 478-481.
218.   D. J. Scott, M. J. Fuchter and A. E. Ashley, *Chemical Society Reviews*, 2017, **46**, 5689-5700.
219.   P. A. Chase and D. W. Stephan, *Angewandte Chemie International Edition*, 2008, **47**, 7433-7437.
220.   D. Holschumacher, T. Bannenberg, C. G. Hrib, P. G. Jones and M. Tamm, *Angewandte Chemie International Edition*, 2008, **47**, 7428-7432.
221.   V. Sumerin, F. Schulz, M. Nieger, M. Leskelä, T. Repo and B. Rieger, *Angewandte Chemie International Edition*, 2008, **47**, 6001-6003.
222.   G. C. Welch and D. W. Stephan, *Journal of the American Chemical Society*, 2007, **129**, 1880-1881.
223.   C. Jiang, O. Blacque and H. Berke, *Organometallics*, 2009, **28**, 5233-5239.
224.   M. Ullrich, A. J. Lough and D. W. Stephan, *Journal of the American Chemical Society*, 2008, **131**, 52-53.
225.   R. Roesler, W. E. Piers and M. Parvez, *Journal of Organometallic Chemistry*, 2003, **680**, 218-222.
226.   M. Reißmann, A. Schäfer, S. Jung and T. Müller, *Organometallics*, 2013, **32**, 6736-6744.
227.   A. M. Magill, K. J. Cavell and B. F. Yates, *Journal of the American Chemical Society*, 2004, **126**, 8717-8724.
228.   L. Greb, S. Tussing, B. Schirmer, P. Oña-Burgos, K. Kaupmees, M. Lõkov, I. Leito, S. Grimme and J. Paradies, *Chemical Science*, 2013, **4**, 2788-2796.
229.   J.-N. Li, Y. Fu, L. Liu and Q.-X. Guo, *Tetrahedron*, 2006, **62**, 11801-11813.
230.   D. Jaques and J. Leisten, *Journal of the Chemical Society* 1964, 2683-2689.
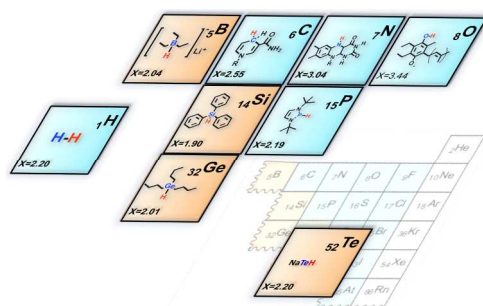
Thermodynamic and kinetic hydricities provide useful guidelines for the design of hydride donors with desirable properties for catalytic chemical reductions.